POLITO SAILING TEAM

*Politecnico di Torino*

*Torino, Italy*

# SuMoth Challenge 2022

*Stage S1 - Design Report*

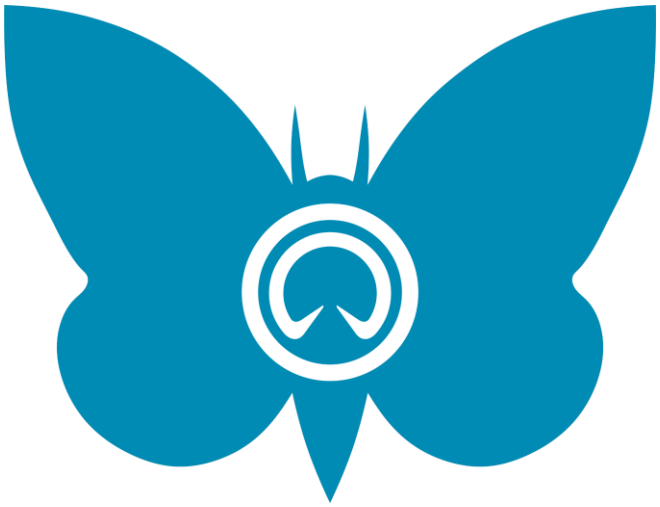

# Abstract

This year, we, as the PoliTo Sailing Team started a new chapter with our moth project named **SULA** for the 2022 edition of the SuMoth Challenge.

Our main goal was to build a new performing and sustainable moth by applying the important knowledge we obtained last year with our project KETH.

The project started in October 2021 with a first stage of evaluating KETH's weaknesses and focusing on finding new solutions. As we learned, the design phase is a key issue of a draft. That's why it took four months in which we planned a rigorous schedule by detailing nearly every aspect of the project. The first manufacturing activities started in February with the production of hull and deck mould.

Even though SULA was developed relatively little time, it brought important innovation both in the design and production processes involved.

The basic concepts that form that backbone of the project can be summarised by three concepts:

- Flight stability
- Sustainability
- Sailor centered

A lot of time was dedicated to research in order to find the best solution to guarantee a stable flight, so that the sailor could concentrate on the race and feel secure while flying. For this reason, two interchangeable control flight systems have been designed: *The Twin Systems* (mechanical and electronic).

The choice of materials and the way the manufacturing processes were conceived were all foucused towards minimising environmental impact, while also considering whether our chosen production methods could be applied on an industrial scale. The concept of the SM$ led to be very useful in the understanding of our environmental footprint during all processes of developing the prototype.

Last but not least, the entire design phase was characterised by a strong collaboration between the designing areas and the sailors, with the common goal of creating a prototype "tailor-made" for the sailor and giving both sides the opportunity to learn from each other.

Throughout this report, these three key points will prove to be fundamental in all phases of this project, and the following sections will go into detail regarding design and manufacturing processes that SULA is founded on.

# Table of contents

# List of figures



# List of tables

# 1 Engineering and Design

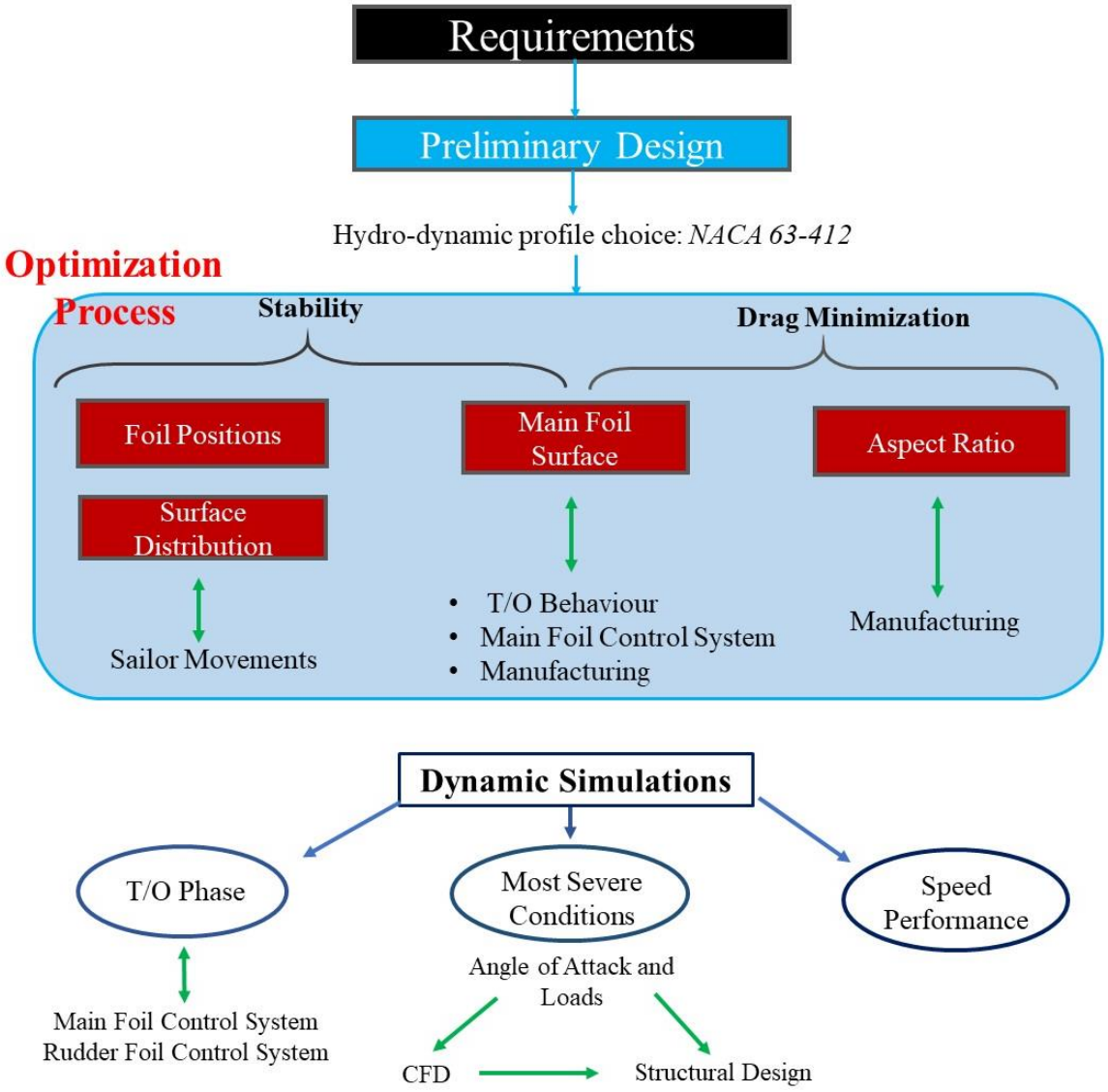


*Figure 1-1: Design logic scheme*

## 1.1 Preliminary design

A month after the end of the last SuMoth Challenge, won with the KETH prototype, the team was excited and ready to start a new experience aware of what good and bad had been done in the last project. This is why the project **SULA** stems from the idea to design and build an innovative and sustainable boat without losing sight of reliability.

The key word that guided the concept during all design phases is **stability**, in accordance with one of the main requirements a hydro-foiling boat must meet. In fact, despite the fact that the helmsman is the main "controller" of the boat, a proper design leads to a reduction of his/her workload. The concept of stability can be summarised as the boat's capability to return to its previous equilibrium conditions following a disturbance. During the regatta, the boat is subjected to several external and internal factors, which can cause it to collapse, such as waves, wind

gusts as well as the sailor movements. However, the requirement of stability, generally leads to a worsening of the maximum speed performance, hence the need to find a balance in order to guarantee a stable and efficient boat at the same time.

For these reasons the preliminary design analysis has been based on the foils' geometry and hydro-dynamic characteristics, and through preliminary performance assessments has been possible to identify some crucial parameters to work on:

- Foil's positions;
- Foil's surface distribution;
- Foil's surface absolute values.

As far as hydro-dynamic profile is concerned, an analysis among several conventional airfoils has been conducted focusing on efficiency and the "stall behaviour", resulting in the selection of *NACA 63-412*. This is due to a good lift to drag ratio and a soft stall angle in line with desired performances.

At this point, an optimisation process began, aiming to find the most suitable boat configuration according to various requirements. These deriving from the objective to maximise both performance and stability, and from manufacturing constraints. This process was founded on the following assumptions based on a benchmark analysis of the most well-known moths:

- Fixed position of the centre of gravity, coming from previous estimations of weights and sailor position;
- Fixed vertical appendages' hydro-dynamic characteristics, resulting in *NACA 0018* for the daggerboard profile and *NACA 0012* for the rudder;
- Fixed vertical appendages' dimensions, coming from a balance among maximum ride height, maximum heel angle and foils' arm with the respect to the centre of gravity;
- Fixed aero-dynamic sail performances, coming from experimental data of Boegle [1].

This resulted in the following. To maximise the pitching moment, the rudder foil is placed at the maximum position towards the stern, while the main foil is closer to the centre of gravity, resulting in less pitching up moment from an increase of lift force. In fact, the main foil generates a large amount of lift due to a greater wetted surface, and even a small variation in the angle of attack is thus enhanced. At the same time, the surface ratio between rudder and main foil amounts to $0.8$ strengthening the latter effect. Finally, as far as foil's surfaces are concerned, there is a significant effect on the performance of the boat during the entire speed range leading to different take-off and maximum speeds. The main foil's surface is $0.15m^2$, a value out of range of the commercial moths. However, following a thorough analysis of the requirements of the subsequent design stages, a decision was made to maintain this value as it leads to a take-off speed of $3\ m/s$ with a less demanding condition for the main foil control system and makes the manufacturing phase more comfortable.

The next step of the optimisation process concerned the requirement of drag minimization. If foil's *wetted surfaces* are fixed for stability reasons, the parameter to act on is the *Aspect Ratio*. It is defined as the ratio between the square of the wing span and the area (or alternatively as the ratio between the wing span and the mean aerodynamic chord) and it strongly affects the lifting and resistance performance of foils:

$$\boldsymbol{AR} = \frac{\boldsymbol{b^2}}{\boldsymbol{S}} = \frac{\boldsymbol{b}}{\boldsymbol{\bar{c}}}$$

$$C_{L_{\alpha_{3D}}} = \frac{C_{L_{\alpha_{2D}}}}{1+\frac{C_{L_{\alpha_{2D}}}}{\pi \cdot AR}} \ ; \ C_D = C_{D_0} + \frac{C_L^2}{e\pi AR} + C_{D_{wv}}$$

By respecting the constraint of minimum chord of $10cm$ for manufacturing reasons, and bearing in mind the "stall prevent condition", the results obtained are:

$$AR_{mf} = 9.35 \quad ; \quad AR_{rf} = 7.16$$

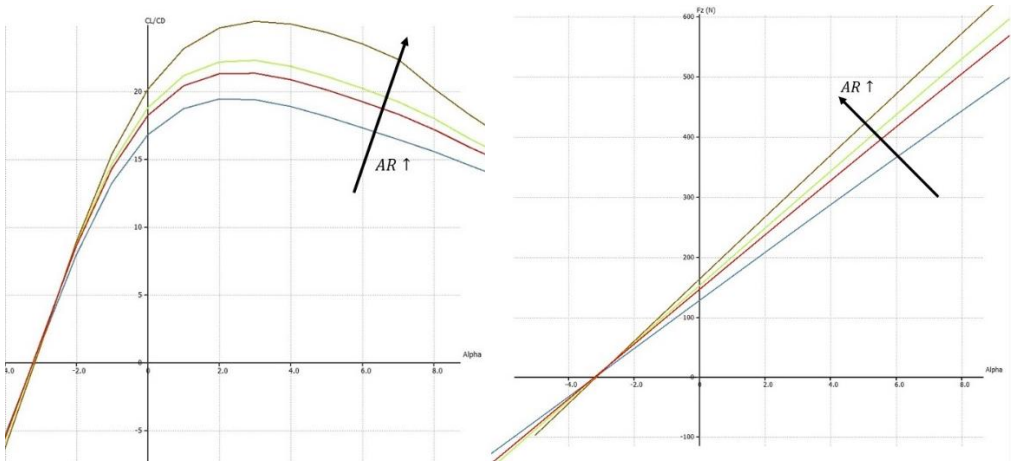


*Figure 1-2: Aspect ratio's effect*

Moreover, the root and tip chords are obtained as a consequence of the mean aerodynamic chord and the taper ratio, strictly related to the sweep angle:

$$c_{root} = \bar{c}\frac{3(1+\lambda)}{2(1+\lambda+\lambda^2)} \; ; \; c_{tip} = c_{root}\lambda$$

| $x_{mf}[m]$ | $S_{mf}[m^2]$ | $AR_{mf}[-]$ | $b_{mf}[m]$ | $c_{root_{mf}}[m]$ | $c_{tip_{mf}}[m]$ | $i_{mf}[°]$ |
|---|---|---|---|---|---|---|
| 1.46 | 0.154 | 9.35 | 1.2 | 0.153 | 0.09 | 4 |

*Table 1-1: main foil's data*

| $x_{rf}[m]$ | $S_{rf}[m^2]$ | $AR_{rf}[-]$ | $b_{rf}[m]$ | $c_{root_{rf}}[m]$ | $c_{tip_{rf}}[m]$ | $i_{rf}[°]$ |
|---|---|---|---|---|---|---|
| 3.8 | 0.126 | 7.16 | 0.95 | 0.18 | 0.085 | 0 |

*Table 1-2: rudder foil's data*

| $L_D[m]$ | $c_D[m]$ | $S_{wetted_D}[m^2]$ | $L_R[m]$ | $c_R[m]$ | $S_{wetted_R}[m^2]$ |
|---|---|---|---|---|---|
| **0.95** | 0.11 | 0.105 | 0.94 | 0.1 | 0.106 |

*Table 1-3: vertical appendages data*

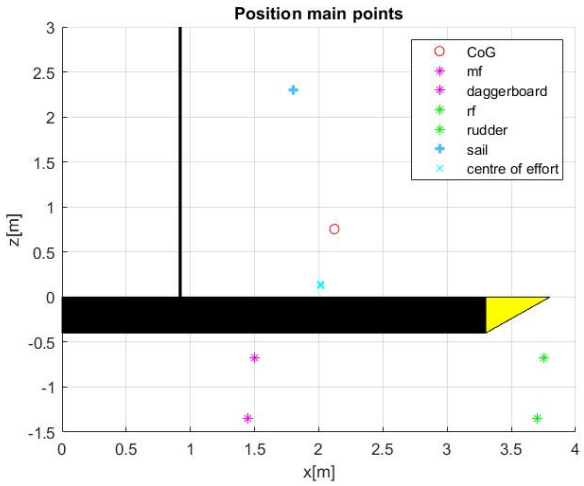


*Figure 1-3: centre of effort positions*

## 1.2 Stability and performance investigation

The previously mentioned optimisation process was based on a simplified static model, taking into account the longitudinal motion and ability to assess the static stability behaviour. However, the resultant design was deeply analysed thanks to the development of a 6DOF dynamic VPP (DVPP). This way, the boat's configuration arose by the optimisation tool while the DVPP allowed for subsequent design choices to be tested and to "predict" their effects into the final performances. The stability concept takes its cue from the aeronautic field theories and it is applicable to the foiling boats, despite some differences. In particular, the longitudinal static stability is evaluated though the derivative of the pitching moment coefficient $C_{M_\alpha}$, while the dynamic stability is based on the linearized dynamic model i.e. on the study of eigenvalues sign.

Considering the overall speed range, from the take-off speed to about $12m/s$, the results show a negative $C_{M_\alpha}$ value, also proved by the pitching moment trend. In particular, following a disturbance causing an increase of the pitch angle, the boat produces a pitching down moment to return to its previous equilibrium condition. The greater the speed the higher the stability because of the increase of the pitching down effects. This occurs due to the rise of foils' drags. The dynamic behaviour is stable too, due to the negative sign of the eigenvalues. The dynamic response is dominated by an oscillatory mode coupled with an aperiodic one, resulting in a damped system which expires its oscillations in less than 10 seconds. Moreover, due to the small magnitude of the fluctuations, the sailor is not called upon to intervene to restore the equilibrium.

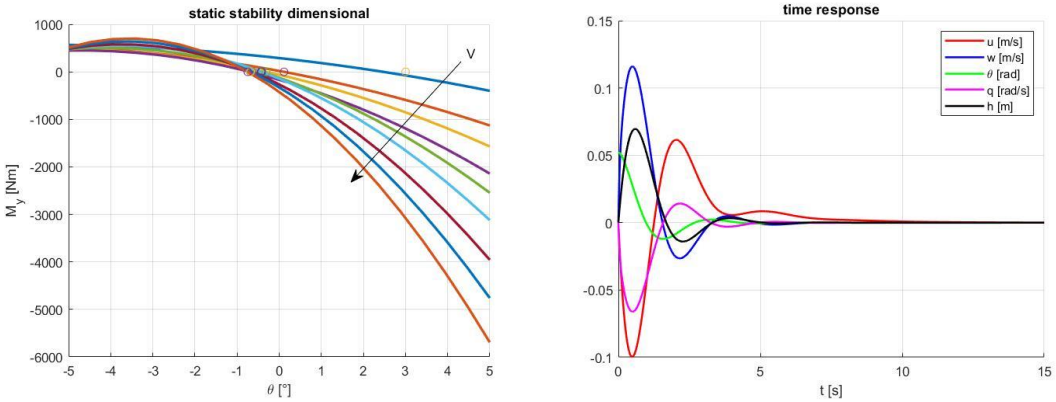


*Figure 1-4:* static and dynamic stability (perturbation of $\vartheta = 3°$)

Having proven the efficacy of the design configuration, an in deep analysis of the dynamic performance was conducted through the DVPP. In particular, for design purposes, this instrument is useful to:

- Provide information to the main foil control system's design in both the take-off and steady conditions;
- Provide a first approximation of expected loads;
- Estimations of top speeds.

For the take off phase, simulations were performed under a true wind speed of $5\ m/s$ and a true wind angle of $50°$, to replicate an upwind take off. First, it is possible to understand how the preliminary design predictions are respected because of the correspondence between take-off speeds. As far as the main foil control system is concerned, it leads to a maximum flap angle of $14°$ at T/O, representing a non-demanding condition and far from the stall angle. As the height increases, the flap reduces its value in order to modulate the lift forces and prevent the boat to jump out of the water. Totally, just after $1.8\ s$ the hull is outside the water, and the steady flight condition is reached in less than $20s$.

Estimating the expected loads is crucial for the structural design. For this reason, further simulations were conducted with more sever conditions of $TWS = 10\,m/s\,, TWA = 100°$ and a heel angle of $\varphi = 20°$. Lift forces come from the classic aerodynamic theory and depends on the lift coefficient, strictly related to the value of the angle of attack. As the dynamic occurs, there is a strong variation in the AoA leading to a consequent change in the lifting performances. At the T/O speed, 85% of the boat's weight is withstand by the main foil due to both a great wetted surface and angle of attack. As the longitudinal and vertical speeds increase, the loads likewise rise due to the dynamic contributions and the added mass effects. In particular, the most demanding point is placed at $5\ m/s$ when the main foil is loaded by about $130\ Kg$, whereas, in order to guarantee the equilibrium, the rudder foil develop the maximum downforce at $4.5\ m/s$. Further detailed simulations are described in section CFD (*1.7.1)*

Finally, to test our top speeds, several simulations were carried out by changing the course and the wind conditions. Results seem to be in accordance with reality, since the top speed is reached in downwind conditions when the sail is almost fully powered. Lower speeds occur in upwind because of the need to balance the strong capsizing moment by depowering the sail.

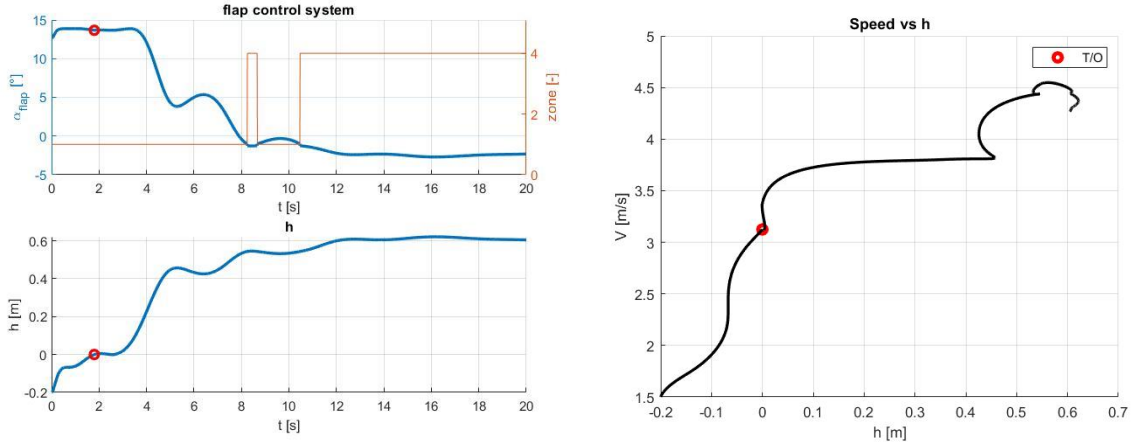


*Figure 1-5:* T/O analysis: flap and speed-fly height correlation

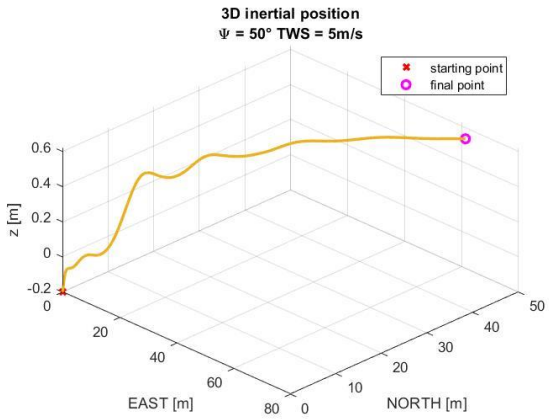


*Figure 1-6:* T/O analysis: 3D visualization

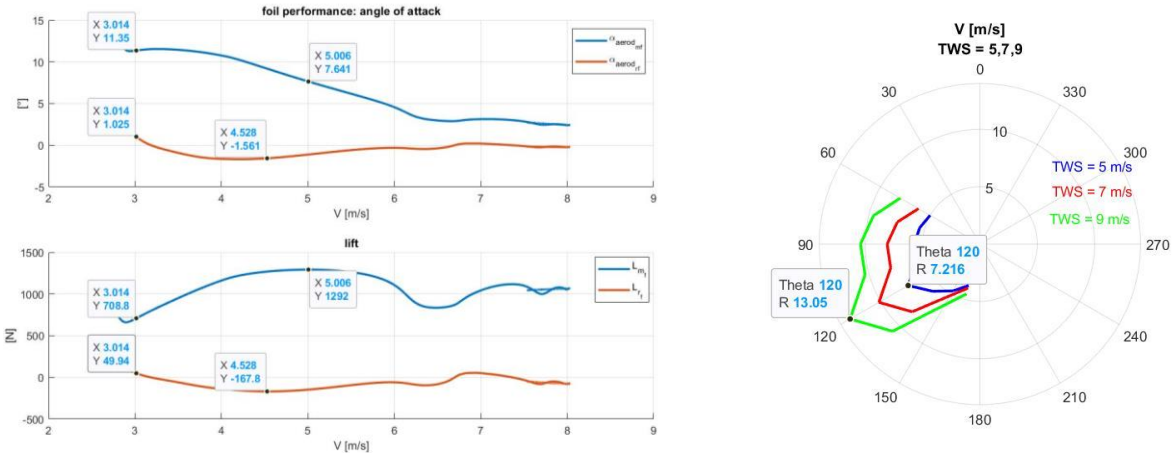


*Figure 1-7:* Loads' analysis (left) top speeds polar plot (right)

## 1.3 Hull design

The first step towards deciding the hull shape design consisted in observing and analysing the commercial moths, evaluating their geometries, construction and behaviour, in order to have the most consistent possible feedback from the sailing community. The following designs were discussed and compared, among others:

- *OneFly*, a good boat to begin one's foiling learning experience;
- *MantaMoth*, which lately has been one of the most advertised and sold moth class boats;
- *Mach2*, which the team had at disposal for practicing moth sailing;
- *Bieker* moth, since it's one of the highest performing projects which main characteristics are low wetted area of racks and high slender ratio with low cross section areas;
- *Bladerider* which as previous generation of the Mach2 by *McConaghy*;
- *Skeeta*, which had a lot of positive feedback about its "sailing qualities" with a design principle which is so simple to look dumb in the intent of maximise water inertia, which leads to have very high natural pitching frequency and therefore dropping the amplitude of the pitch response of the boat. This feature in the latest years, interestingly, can be noted to be quite a trend among different classes.

Beyond basic literature, particular attention was given to [2]**,** where practical considerations about moth sailing are made, and a huge variety of reference values are presented. With critical analysis, the designs listed above were taken into account while defining sizes and parameters of SULA.
The Team's idea behind the hull design aimed towards making take off phase easy, improving pitching stiffness and generally providing an abundant buoyancy almost compatible with displacement-type sailing. For these reasons, *OneFly* was taken as preferred reference boat.

To design the hull a NURB surface was manipulated with the software Maxsurf because it can automatically compute the most of geometric coefficients and values which are relevant to the purpose.

| | | |
|---|---|---|
| **Volume (displaced)** | 0,107 | $m^3$ |
| **Displacement** | 107,2 | $kg$ |
| **Draft Amidships** | 0,2 | $m$ |
| **Immersed depth** | 0,128 | $m$ |
| **WL Length** | 3,355 | $m$ |
| **Wetted Area** | 1,635 | $m^2$ |
| **Prismatic coeff. (Cp)** | 0,647 | |

*Table 1-4: Hull design data*

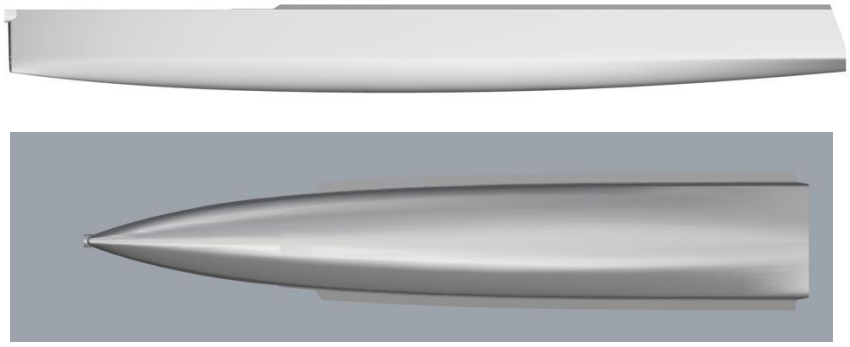

*Figure 1-8: Hull design shape*

## 1.4 Deck design

Since the flat deck could have created additional difficulties for the sailor during manoeuvres, when moving from one wing to the other, a concave deck as opted for. This can also be seen as a soft junction into the wings, as the angle at which the external edges rise coincide with the wings' angle themselves.

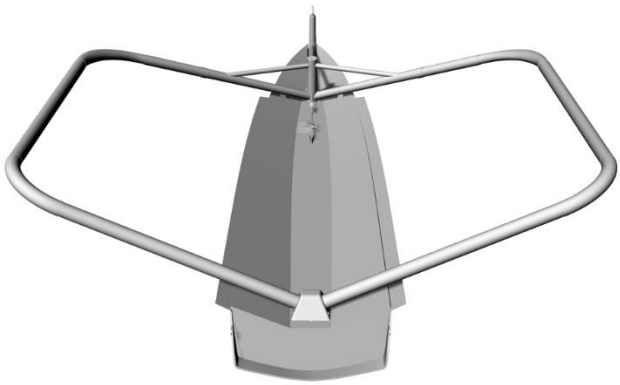

*Figure 1-9: deck CAD*

## 1.5 Hull, deck: internal structure

The internal structure is one of the crucial parts of the boat, since it allows the hull and the deck to withstand the loads originating from the sailor's weight and the rig's tensions. The design consists of:

- A front spar, from head to centreboard, to withstand the bending moment produced by the forestay tension.
- A back spar, to counteract the rudder foil's lift.
- A front rib to set the spar under the mast.
- A back rib to counteract the moment acting on the wings.
- The upper stern to attach the gantry with the back spar.

To constrain the rotation towards the bow, a bowsprit/strut bowsprit solution was adopted. One of the main aspects was deciding how to link the mast base and wing attachments to the internal structure in order to unload the deck. After discarding the proposal of "through deck tubes", a simpler solution in terms of construction, nonetheless, just as effective, was opted for: using steel plates bound by screws to the internal structure, and by screws to the mast base and the wings bar. Regarding the tube in which the bowsprit will be housed, it was decided to tie it to the rest of the hull through a wrapping on the flange of the extreme bow with rowing.
For the rear wing attachments, initially, anchoring the tubes only to the hull flanges was considered. Regardless, in order to pursue the aim of leaving the deck as unloaded as possible, true decision was made to make a part of the spar protrude through the deck and fixing the tubes directly to trough 3D printed holders.

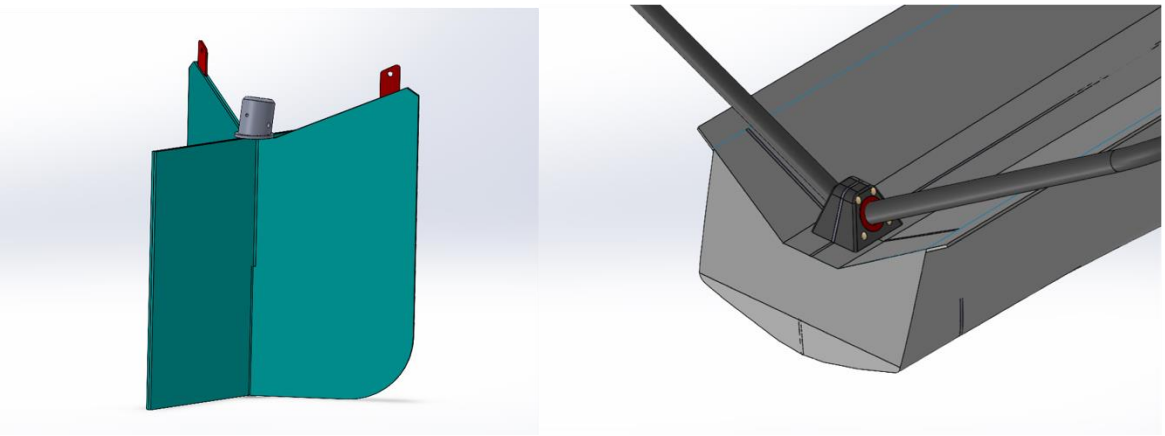

*Figure 1-10: Internal structure: mast base and rear wing attachment*

### 1.5.1 Structural model

The dimensioning was carried out by a detailed structural analysis where real conditions were simulated. In particular, the load of the sailor is supported by the wings which, through the connection to the mast, transfer the load to the front rib and spar; similarly, the forestay tensions. On the other hand, on the stern, the main load comes from the rudder foil's hydrodynamic forces which are transferred through the gantry's structure.

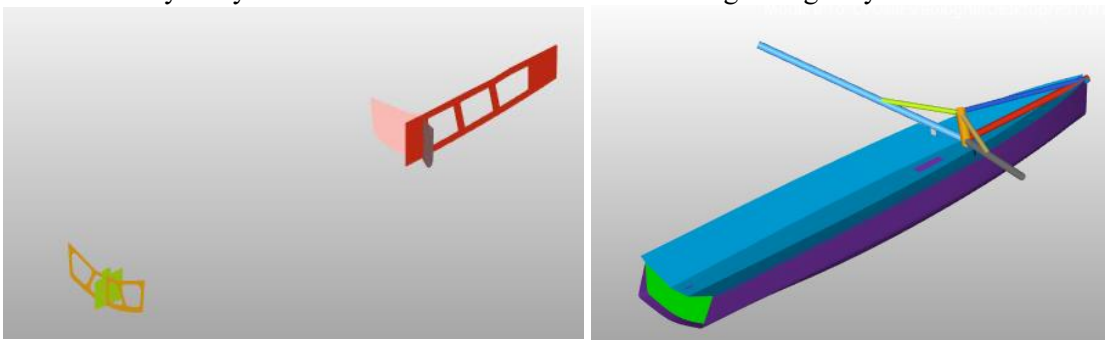

*Figure 1-11: hull internal structure - hull, deck, reinforced tubes*

As far as loads are concerned, they stem from the two most frequent regatta conditions:

- Steady flight: sailor is placed on the external wing to balance the capsizing moment. This load case is the most critical for the hull, the tie rods, and the internal structure.
- Displacement regime: sailor is standing up on the deck.

The load's magnitudes, shown in the table below, are obtained from a tension load cell for the forestay and the boom vang, from fluid dynamic simulations and from geometrical considerations. A safety factor is also considered addressing the uncertainty of their values.

| **Load** | **Magnitude [N]** | **Point of application** |
|---|---|---|
| Forestay tension | 2500 | Head deck |
| Sailor weight | 1600 | Wings |
| Lift of the centreboard foil | 1020 | Centreboard rigid RBE |
| Lift of the rudder foil | 480 | Rudder rigid RBE |
| Mast compression | 5500 | Mast |
| Boom vang | 7500 | Mast |

*Table 1-5: Loads for Hull structural analysis*

Then, composite materials were chosen to obtain adequate stiffness while maintaining low weight, using a sandwich structure for hull and deck, while the internal structure was designed using ***okumè wood***. While maintaining the objective of project sustainability, skin and core of the sandwich were obtained from leftover materials from prior team activities.
In order to minimize the sandwich weight, all possible stratifications have been compared and, eventually, a sandwich with a core of ***balsa wood*** 6,4 *mm* thick and skin of ***TWILL basalt fiber*** $0°/90°$ for the hull was chosen, while for the deck a sandwich of ***PET*** 10 *mm* thick reinforced with ***twill basalt***.
Furthermore, the deck presents a sandwich spar laminated on the deck to decrease substantially the displacement, without adding too much weight. All ***basalt/S glass fiber*** reinforcements were defined by the simulation results, which they brought to the following stratifications. However, more details on the materials are reported in the table.

| **Material** | **Mechanical properties** | **Magnitude** |
|---|---|---|
| UD Basalt | $E_1$ | 36115 [MPa] |
| | $E_2$ | 8713 [MPa] |
| | $v_{12}$ | 0.322 |
| TWILL Basalt | $E_1$ | 31449 [MPa] |
| | $E_2$ | 31449 [MPa] |
| | $v_{12}$ | 0.15 |
| Balsa wood | E | 1680 [MPa] |
| | v | 0.35 |
| S-Glass | $E_1$ | 43680 [MPa] |
| | $E_2$ | 9130 [MPa] |
| | $v_{12}$ | 0.194 |
| Okoumè | E | 7800 [MPa] |
| | v | 0.02 |
| PET | E | 120 [MPa] |
| | v | 0.3 |
| Steel | E | 210000 [MPa] |
| | v | 0.3 |
| Cork | E | 28 [MPa] |
| | G | 5.9 [MPa] |

*Table 1-6: hull, deck, internal structure materials*

Finally, a linear static analysis was performed to investigate stresses and displacements. Results obtained with *OptiStruct* show that the most stressed part of the boat is the mast foot. Displacements are small compared to the dimensions of the boat and stresses are much lower to the yield stress.

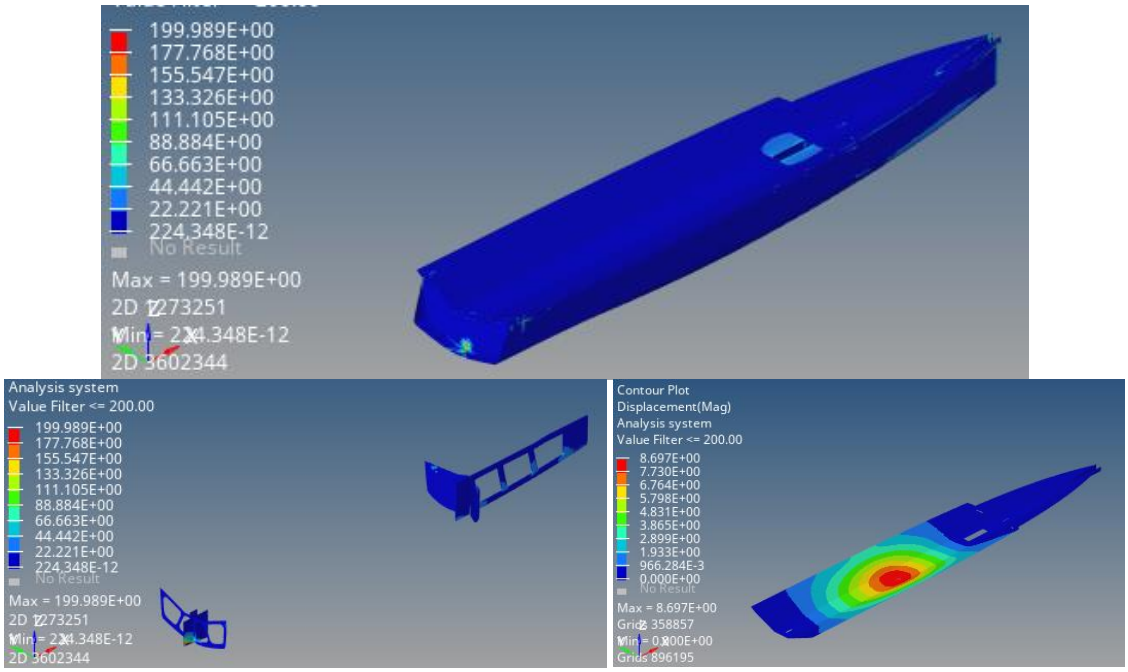


*Figure 1-12: stress of hull and deck (load case 1), stress of internal structure (load case 1), displacement of deck (load case 2)*

## 1.6 Mould design

For this year's competition, the team thought of a way to produce the moulds without heavily impacting the environment, since usually it is one of the main causes of pollution in the production of a boat.

### 1.6.1 Hull mould

Since the precision on the hull mould was important, it was decided to mill it; the idea was to make it reusable in order to minimize the waste of material that a disposable mould would have resulted in. The initial idea of a mold milled from a single block was discarded and a division into five blocks was opted for, in turn divided into various slabs that were then glued together. Thanks to this method we were able to save around 50% of the initially estimated volume of material and to significantly reduce the milling hours. This method could also be used in a company view where, although processes are slightly more complicated, it could prevent heavy pollution and minimize costs of production (in materials and milling hours) without spoiling the final result.

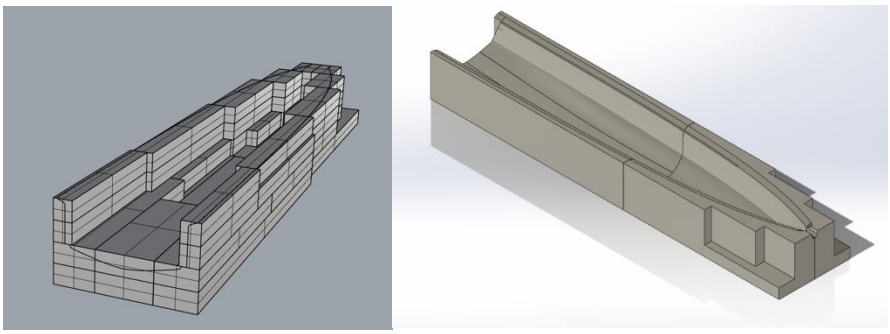

*Figure 1-13: Hull mould*

### 1.6.2 Deck mould

A similar method to that of the hull's mould was adopted for the deck's mould, to make it reusable for future laminations. This mould is divided into two different parts which were then glued together. The stern part, which is characterized by an almost linear geometry with minimal curvature, is composed of 8 sixths arranged vertically, held in position by a central spar. To create the surface of the mould then to be laminated on, a $4mm$ plywood sheet was used, properly cut with templates, and fixed in position with nails.
The bow part has a more complex geometry due to the presence of the bowsprit and the end of the flange. For this reason, it was decided to mill it entirely from a $100\ mm$ thick block of expanded polyurethane foam scrapped from the assembly of the hull's mould.
The two parts were then aligned with the help of the central spar and were glued together. The gap between the two then filled with ultra-fine filler.

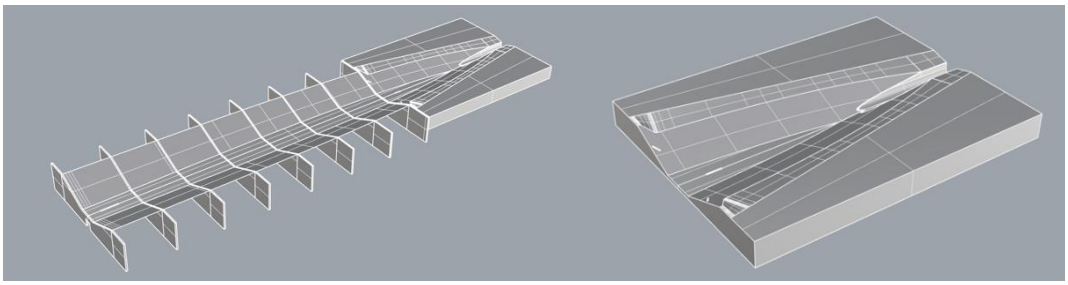

*Figure 1-14: Deck mould*

### 1.6.3 Deckhouse

The deckhouse must carry out the task of always keeping the electronic control system dry. In order to design something functional and aesthetically appealing, the first option was centred around a curvilinear shape; however, considering the future maintenance operations, the need of an afterpeak led us to a straighter profile, in order to facilitate its waterproof application. In fact, the room in the back of the deckhouse is extremely small, due to the presence of the mast foot and the wings attach, leading to the afterpeak necessitating a lateral position, thus needing to be designed as flat as possible. This way, there was enough room for all the systems and for a waterproof **"control window"**. This shape not only solves every project constraint, it also facilitates the entire construction process.

*Figure 1-15: deckhouse CAD*

## 1.7 Foils

### 1.7.1 Computational models for CFD analysis

The detailed design of foils stems from the results of the preliminary stages where geometrical dimensions are defined as well as predicted loads. Therefore, a CFD (Computational Fluid Dynamic) analysis is one of the focal points of the foil's design from which results are then provided to the structural and control system areas. For example, contributed to:

- Validation of the goodness of the preliminary assessments;
- More accurate loads' estimations;
- More accurate pressure distributions;
- Flap hinge's moment estimations.

Starting from the CAD model, the pre-processor *BETA-CAE ANSA* was used to prepare the surface topology for the CFD simulation process that followed. Then, the commercial software *STAR-CCM+* was used in order to define coherent physical models and create refined meshes capable of outputting highly exploitable results. As far as the physical model is concerned, it is composed by the following characteristics most suitable for simulated conditions:

| Physical model |
|---|
| **Steady model** |
| **Liquid with a constant density and viscosity (water)** |
| **Turbulence model K-ε** |
| **Segregated-flow model** |

*Table 1-7: Physical model for CFD*

The mesh is based off of a parallelepiped block of fluid (water) in which the foil is embedded near the vicinity of the water line. In addition, four control volumes were added in order to achieve improved computational results in certain crucial areas of the mesh depicting: the wake, the fluid volume in the direct vicinity of the foil, the tip extremity and finally, the leading edge. Furthermore, a prism layer was used, composed of 8 prism layers for a total thickness of $4mm$ to accurately compute field on the frontiers of the foil. The total number of cells for the final mesh was 6409849.

Moreover, the retained boundary conditions are the following:

- *Velocity inlets* for are all boundaries of the fluid except the exit;
- *Pressure outlet* for the exit boundary;
- *Wall* for the frontiers of the foil.

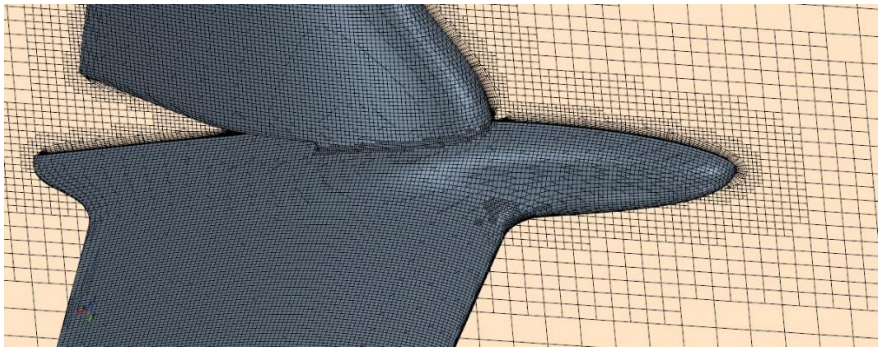

*Figure 1-16: Model refine mesh*

Two of the most important simulations for the next design stages are described below. The first one regards the complete T-foil configuration under the most demanding conditions, estimated by the previous dynamic simulation:

- Navigating speed of 5.2 $m/s$;
- Angle of attack of 7.5°;
- Leeway angle of 3° (coming from the left of the figure).

It is possible to understand how the pressure distribution is in line with the expected behaviour resulting in a stagnation point on the left side of the daggerboard, as well as a clear bending moment on the foil.

Furthermore, a step closer to the reality has been made by simulating the flap deflections. For example, the take off condition is tested by imposing an angle of 14° at 3 $m/s$ resulting in a lift force of 863 $N$, in accordance with the preliminary tested conditions.

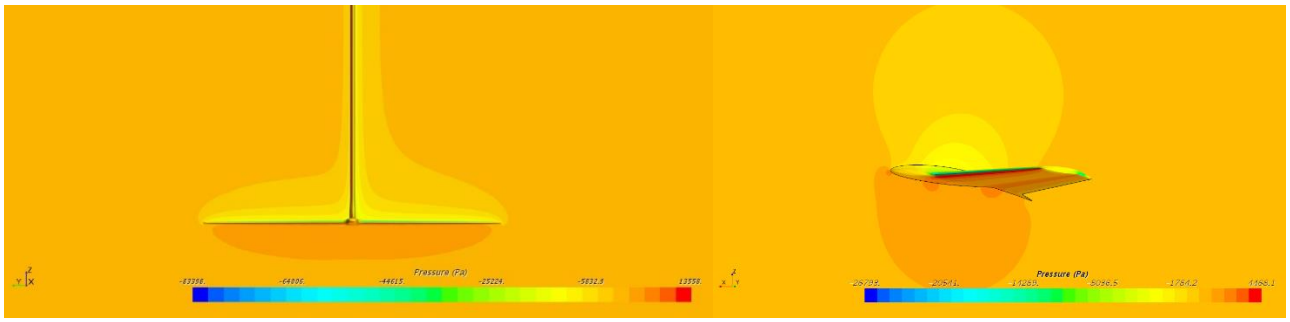

*Figure 1-17: Pressure field for centreboard T-foil and main foil with flap angle at 14°*

### 1.7.2 Finite element structural analysis

Once the geometry and hydro-dynamic characteristics of foils and vertical appendages were defined, the structural design commenced. The process follows the model-based approach, by shaping the right modelling according to the various analysis that must carried out, and aims to find the optimum balance among mechanical resistance, performances and lightness.

After importing the geometries into HyperMesh, the mathematical model was created to represent the real connections, conditions and loads associated with the designed T-foils' configuration.
In particular, the constraints of the model were considered by binding nodes representing the interface between the appendage's verticals and the hull. The link between the vertical appendage and the foil was considered by using a **non-linear contact formulation**, so that the nodes of the interface are bound to move together and transmit forces. A detailed contact modelling was developed, tested and calibrated during the whole project period.
In order to choose the most critical working conditions under a structural point of view, continuative interface and dialogue with dynamic and overall design divisions was maintained. The maximum appendages' hydrodynamic loads' conditions during the operative life are listed in Table 1-8 and loads were imported from the previous CFD analysis. However, to account for dynamic effects, an appropriate safety factor (>2) was applied.

| | **Centreboard** | **Rudder** |
|---|---|---|
| Navigating speed | 5.2 m/s | 4 m/s |
| Incidence | 7.5° | -4° |
| Leeway angle | 3° | 3° |

*Table 1-8 - Operative conditions used for structural design*

As far as materials are concerned, CFRP *(Carbon Fiber Reinforced Polymer)* was the choice adopted for to achieve the highest structural resistance. In addition to CFRP, a filler foaming with a density of $0.25\ g/cm^3$ was used to fill the cavities of the appendages. The CFRP properties are listed in the table below.

| ***Mechanical property*** | ***Symbol*** | ***Magnitude [MPa]*** |
|---|---|---|
| ***Young modulus*** | *E1* | *150000* |
| ***90° Young modulus*** | *E2* | *8190* |
| ***Shear modulus*** | *G12* | *15690* |
| ***Tensile strength*** | *Xt* | *1890* |
| ***Compressive strength*** | *Xc* | *1200* |
| ***90° tensile strength*** | *Yt* | *70* |
| ***90° compressive strength*** | *Yc* | *20* |
| ***In-plane shear strength*** | *S* | *50* |

*Table 1-9 - CFRP Properties*

The analyses that have been set up are:

1. *Non-Linear quasi static analysis:* for the centerboard and rudder assemblies, necessary in order to study maximum stresses and to decide which layering to consider for component fabrication. Non-linear analysis was performed in order to investigate contact forces and status in the joint between vertical appendages and foils.
2. *Linear buckling analysis:* for the vertical centerboard and rudder. This is performed because compressive loads for high aspect ratio's components are very dangerous.

These resulted in: the structure of the appendages being subdivided in main plies and smallest reinforcements such as to optimize the material contribution. For the foils, besides three entire plies (a carbon twill, a $+/-$ 45° carbon biaxial and a UD carbon ply) two tighter and shorter plies are used to enhance bending behaviour (UD carbon plies) and two central reinforcements are used to improve overall resistance (+/- 45° biaxial plies) and torsional behaviour (one UD ply oriented by 90° w.r.t the foil longitudinal direction).
Stratifications that meet the requirements are resumed in Table 4. Plies are divided into main plies (covering all the appendage) and reinforcement plies (covering just parts of reinforcement).

| Centreboard vertical | Centreboard foil | Rudder vertical | Rudder foil |
|---|---|---|---|
| | | | |
| | | | |
| | | | |
| Large | Large | Large | Large |
| Thin | Large – no flap | Large | Large |
| Joint | Thin | Thin | Thin |
| Joint | 90° centre | Large | 90° centre |
| | Joint | Thin | Joint |
| | Joint | | Joint |

| | |
|---|---|
| / | UD carbon 600 g/m2 |
| BIAX carbon 200 g/m2 | UD carbon 400 g/m2 |
| BIAX carbon 200 g/m2 reinforcement | UD carbon 600 g/m2 reinforcement |
| TWILL carbon 220 g/m2 | UD carbon 400 g/m2 reinforcement |

*Table 1-10: T-foils stratifications (with legend on the side)*

All analyses were conducted using *Altair Optistruct* solver.

- *Nonlinear quasi-static analysis*: results show that the most stressed part are foils' fuselage sides and verticals' joints, because of bending moment. Contact forces and locations are in expected ranges and shows the expected behavior. Stress concentrations can be observed in particular in geometry-variations areas and in correspondence of ply stack changes due to the presence of local reinforcements. Displacements show a rigid behavior of the whole appendages, in line with the objective to have high stiffness for boats' stability.

- *Linear buckling analysis*: centerboard's results turn out a BLF (Buckling Load Factor) associated with a critical buckling load of 7998.91 $N$, which returns a safety factor of around 6.1 compared to expected loads. Instead, for the rudder, output BLF is associated with a critical buckling load of 1067 $N$, which returns a safety factor of around 6.4 compared to expected loads.

It is worth remarking that the difference of critical loads' magnitudes between the centreboard and rudder's verticals should be attributed to different boundary conditions.

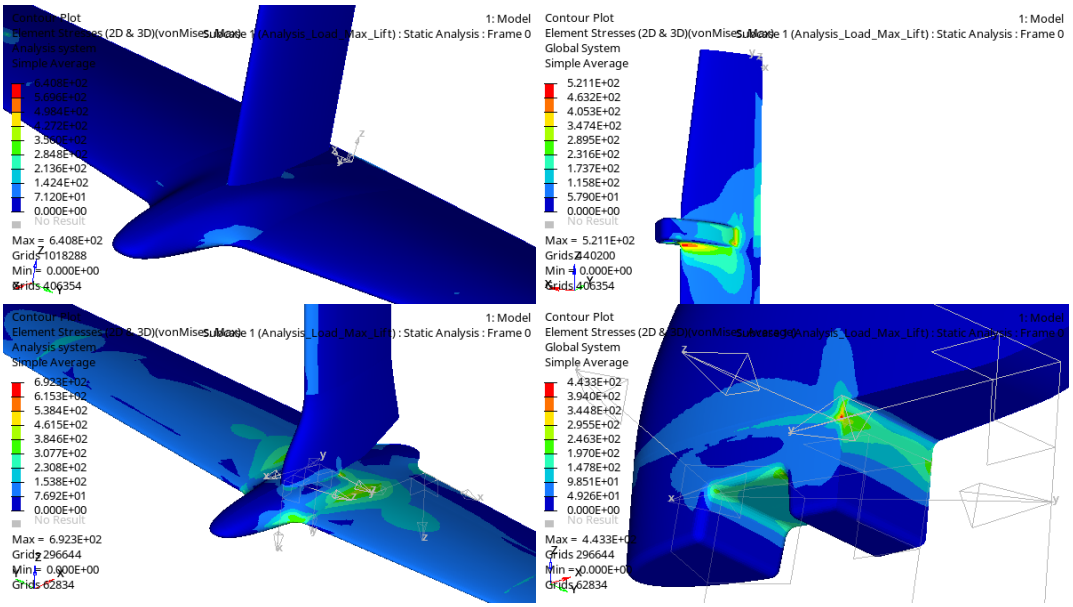


*Figure 1-18: structural analysis results: rudder and main foil (left) rudder and centreboard (right)*

According to the Foiling SuMoth Challenge official rules, a weight estimation was conducted to determine the exact percentage of CFRP used in the fabrication of appendages. The following input parameters were considered:

- Foil surfaces ($\boldsymbol{S_a}$) and volumes ($\boldsymbol{V_a}$) evaluated through CAD measurements;
- Fibers specific weight from the supplier datasheet ($\boldsymbol{w_f}$);
- Ply thickness $\boldsymbol{t_p}$;
- Absorption factor $\boldsymbol{a}$ which gives an average of $55\%$ $R.C.$ (resin content by weight) as set out in the rules;
- Filler foaming density $\boldsymbol{\rho_d}$ .

Considering the stratification obtained from the structural analysis, the number ($\boldsymbol{n_p}$) and thickness of the plies were used to compute the volume occupied by the CFRP, it is possible to obtain the volume to be filled with foaming ($\boldsymbol{V_{fil}}$). The following equations are considered to compute the total CFRP weight and results are shown in the table.

Composite weight: $w_{CFRP} = S_a n_p w_f a$
Composite volume: $V_c = S_p n_p t_p$
Filler resin volume: $V_{fil} = V_a - V_c$
Filler resin weight: $w_{fil} = \rho_d V_{fil}$
Appendage weight: $w_{ap} = w_{fil} + w_{CFRP}$

| | **Centerboard vertical + foil** | **Rudder vertical + foil** |
|---|---|---|
| **CFRP weight [g]** | 2.781,00 | 1.984,58 |
| **Foaming weight [g]** | 703,67 | 531,95 |
| **Total weight [g]** | 3.516,79 | 2.549,15 |
| **CFRP max weight [g]** | 2.813,43 | 2.039,32 |

*Table 1-11: weight estimation*

Finally, results showed margins for possible future improvements. In particular, a difference between stress statuses of various plies is observed, and this led the team to the research for a design involving basalt fibre and CFRP.

## 1.8 Wings and Rig

Moving on to the wings, a traditional design was chosen, composed by tubes and tramps where the front wing bars attaches are connected to the mast base in order to guarantee a better stiffness in the most stressed part of the boat. Wing angles were determined by comparing different commercial moths resulting in a final choice of a 23° angle to allow for comfortable positioning for the sailor while conducting the boat heeled and during manoeuvres.
Due to uncertain position of the line control system, two laminate plates, where all the blocks and stoppers could be fixed, was designed; this way blocks and stoppers can be moved to optimize the lines without spoiling the deck.

SULA is designed to have both a traditional rig and a wing sail rig provided by Advance Wing Systems [5].

## 1.9 Main foil control system

*Figure 1-19: main foil control system overview*

One of the crucial components of a moth's design is the **main foil automatic control system**, because it allows the boat to reach and maintain the desired right height, as well as guarantee the stability of the boat flight. The main purpose of SULA's project consisted on deeply studying and engineering the flight automatic control system because it is synonymous of research and innovation, milestones of the competition.

This is why, the team has pushed itself to the limit by designing and building two control systems (*the twin systems*): one mechanical and other completely electronic. In line with the reliability and 'easy-to-use' requirements, the main challenge was to integrate properly the two of them and make them easily interchangeable.

As it is known, the **main foil control system** receives the flight height as an input and regulate the amount of lift by moving the trailing edge flap. The identification of the following parameters makes it possible to clearly describe the control system's operating logic and the adjustments that can be applied for different racing strategies. It is worth noting that the design of *the twin systems* stems from the need to match the flap movements coming from the previous design stages to allow the boat to reach the desired performance.

- Flap angle: $\Delta flap$
- Crank transmission ratio: $i$
- Offset adjustment: $\Delta offset$
- Bow mechanism translation: $\Delta x$
- Wand angle: $\Delta wand$
- Wand's length: $\Delta L$
- Fly height: $\Delta h$

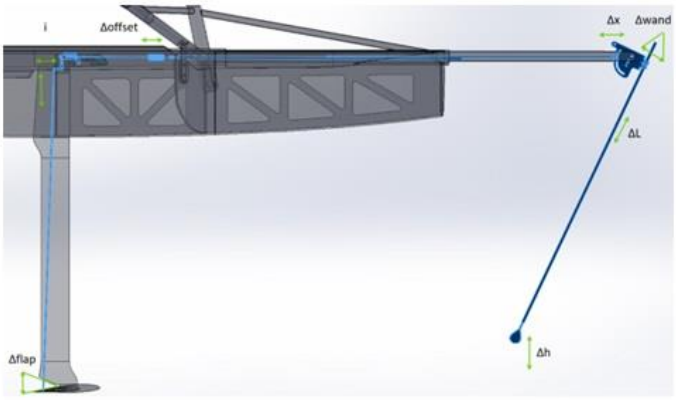


*Figure 1-20: identification parameters*

### 1.9.1 Mechanical system: performance

Being aware of last years' experience, the design started with a deep study of the different available control systems on the moth market. The final choice fell upon the '**Bugscam**' for several reasons:

- The possibility to "customize" the curve of the plate in order to decide the appropriate relation between the height and the angle of the flap, according to different regatta scenarios or sailor needs;
- The presence of the bowsprit permits to get earlier information about disturbances due to the waves;
- The ease to integrate the bow sensor necessary for the electronic system.

With reference to the work of Boman [3] and the article Avalonsails [4], the concept is based on having different sensitivities of the flap angle according to the wand angle variation, i.e. fly height, to avoid the gearing setting and reduce the sailor's workload. In particular, the sensitivity is defined as the ratio between the vertical translation of the rod and the angle swept by the wand: $sensitivity = \frac{z}{\alpha_{wand}} \left[\frac{mm}{^\circ}\right]$.

After several iterations and following the guidelines derived from the preliminary design, the sensitivity is chosen to allow the craft to reach the steady state flight as quickly as possible, and to descend rapidly after the occurrence of a disturbance, through a "back-up" zone capable of immediately reducing lift, thus preventing the craft from jumping out of the water. Specifically, the plate was divided into five zones:

- The first **two zones** refers to the take off phase. A linear trend can be observed, gradually increasing sensitivity. This means that at low rides the flap angle is almost constant and close to the maximum value;
- The **third zone** is represented by the maximum sensitivity. It can be used as steady zone if severe conditions occurs, such as intense waves. In particular the helmsman decides to fly lower and wants the system to be reactive;
- The **fourth zone** is equivalent to the third zone during smoother conditions. In fact, it is possible to fly higher and neglect the effect of small disturbances;
- The **fifth zone** is defined as the "back-up" because, if the ride height is too high, e.g. due to strong disturbances, the flap must move quickly to generate sufficient depower and bring the boat back to the desired height.

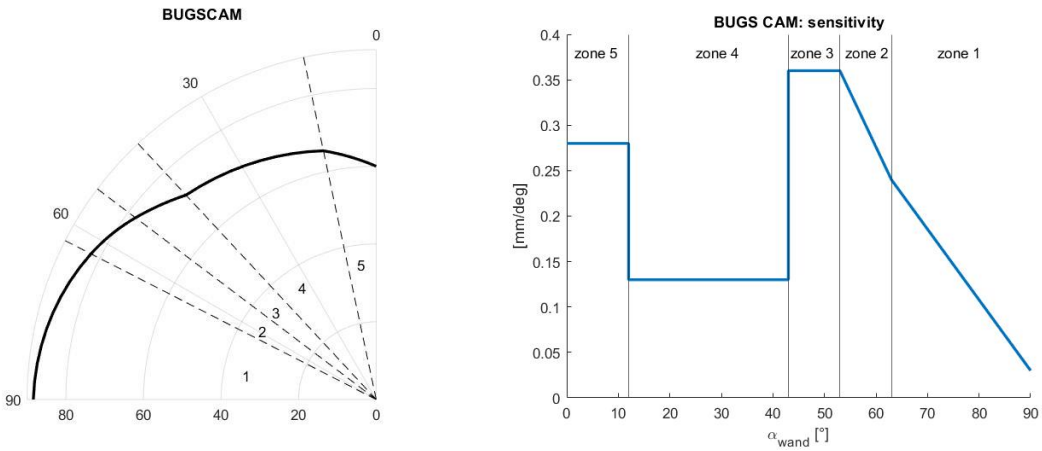


*Figure 1-21: BUGSCAM: zones definition and sensitivities*

Finally, the angle of the flap is strictly correlated to the vertical translation with a simple geometric law, depending on the distance between the rotation hinge and the rod anchor point, as well as the wand angle is linked with the ride height through the length of the wand:

$$\alpha_{flap} = \sin^{-1}(z/l_{flap}) \qquad \alpha_{wand} = \cos^{-1}(z/l_{wand})$$

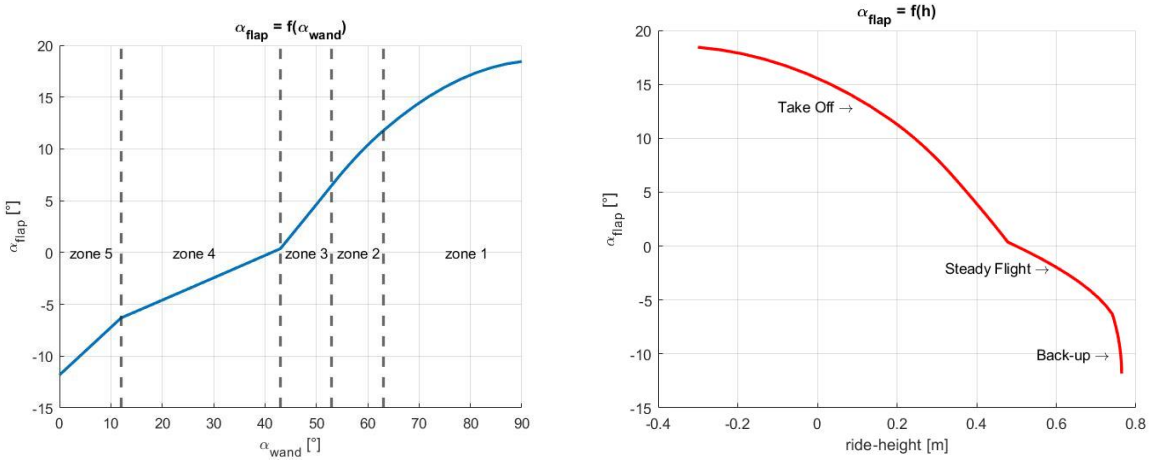


*Figure 1-22: BUGSCAM: flap angle function*

Furthermore, to prove the efficacy of the design, a dynamic simulation was carried out, by simulating a disturbance in the fly height. It is clear that, the steady flight is guaranteed by the **zone 4**, while the system switches to the **"back-up" zone** as the craft flies higher. Similarly, once the boat tends to go down, the **third zone** is activated to restore the equilibrium condition.

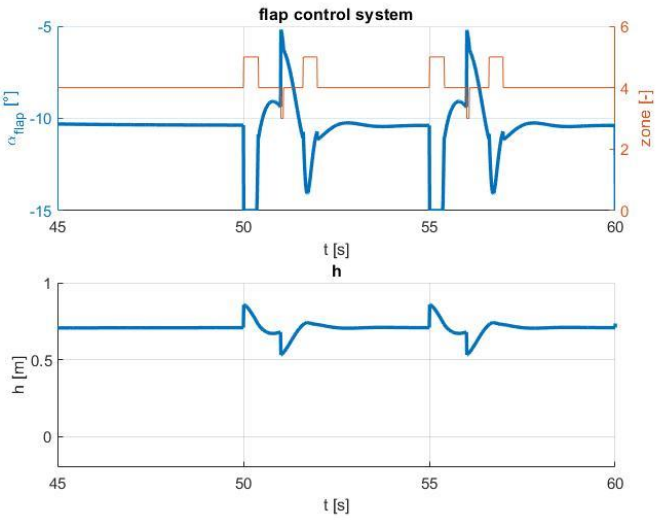


*Figure 1-23: BUGSCAM: response following a disturbance of $z = 0.15m$*

### 1.9.2 Mechanical system: adjustments

With a view to an easy-to-use system, adjustments are fundamental to allow the sailor to manage the control system according to various regatta conditions. This way, the design point is easily switched and the system can continue to operate with the same performances. The two adjustments it was decided to integrate are the **offset** and the **wand length**.

The **offset** is responsible for changing the desired ride height, without changing the sensitivity of the system. In particular, offset lengthens or shortens the transmission rod causing a variation in the flap angle. For example, in downwind courses, the increase of speed is the main factor towards producing enough lift force, therefore the offset tends to assume less value, leading to a lower flap angle.
Resuming the effect of the offset can be analysed as follows: assuming the same speed, with the offset is possible to get different height with the same flap angle.

As far as **wand length** is concerned, it leads to a different flap response with a same input, in order to get a more or less responsive boat. In particular, it is clear that a shorter wand provides the boat to stay closer to the surface of the water, which includes a different response: the boat is globally more sensitive as the angle of the flap changes more quickly, and vice versa.

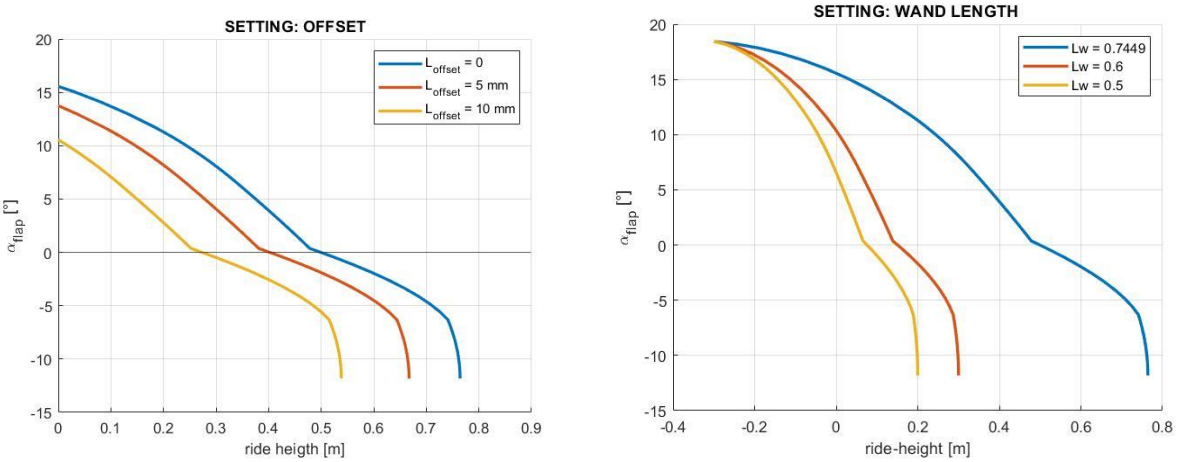


*Figure 1-24: adjustments of OFFSET and Wand length*

### 1.9.3 Electronic system

Firstly, this solution avoids the mechanical measurement of the height, relying on both ultrasonic sensors and an IMU[1]. In particular, the sensing system is composed by:

- 3 **waterproof ultrasonic sensors**, mounted: one at edge of the bowsprit, and the other two at stern, to the left and right extremes of wings;
- **IMU**, which allows to retrieve the spatial orientation of the boat.

By mounting sensors on the edges it is necessary to take into account the inclinations of the moth around $x$ and $y$ axes (roll and pitch respectively). To solve this problem, a sensor fusion approach with IMU coupled with the three ultrasonic sensors was adopted. This way, it was possible to compensate the sensor's errors while being aware of the boat's attitude. However, in order to consider the boat as a flat plane, offsets in the vertical $z$- axes are added to reset the difference among the mounted sensors' positions.
For instance, considering only *UTR 1* (UlTraSonic sensor) and knowing the pitch angle retrieved from the *IMU* and the distance from it (*UTR1 BNO DISTANCE*), with a simple trigonometric calculation is possible to know the impact of the attitude on the sensors' measured data.
By applying these principles to all the sensors it was possible read the heights of the boat as all the sensors were on a flat surface. This way the three adjusted heights, ideally, can retrieve the same distance from the free surface. An average of the three heights is then computed, to reduce the differences coming from the waves.

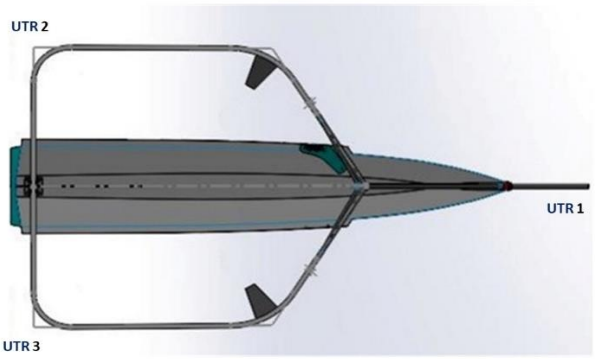


*Figure 1-25: Sensors' positions*

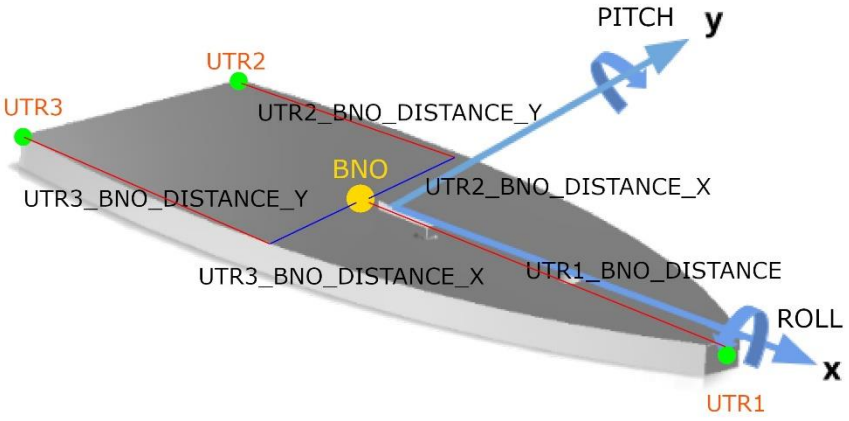


*Figure 1-26: IMU acquisitions*

[1] IMU stands for Inertial Measurement Unit and is an electronic device that measures and reports a body's specific force, angular rate and orientation of the body, using a combination of accelerometers, gyroscopes, and sometimes magnetometers.

With the output of the "height acquisition system", the control loop is closed and an error between the target height and the current one is calculated. At this point a **PID** controller (Proportional, Integrative, Derivative) aims to elaborate this error and provide the right flap angle. The physical actuation is performed through a high torque servo motor, whose angle is changed acting on the duty-cycle of its control signal.

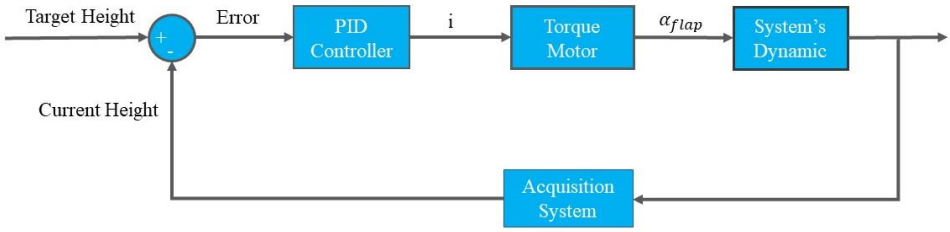


*Figure 1-27: Electronic control system's model*

In order to test and tune the controller parameters, the dynamic model, integrated with the motor model was used. However, future fine gain tuning will be carried out with experimental tests.
The brain of the system is the *STM32 microcontroller* who manage the inputs and elaborate the control law by governing the electrical current on the torque motor. Moreover, a RFID card reader is added to the target height and a buzzer to know the currently selected one.

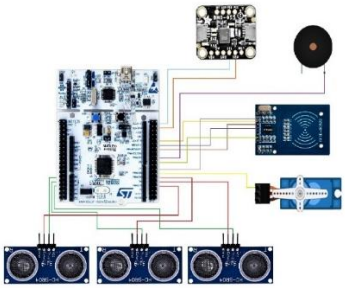

*Figure 1-28: microcontroller*

### 1.9.4 Constructive choices

As a result of meticulous study of the components, tolerances and jokes on the control line couplings, the final tensioned system is presented.

1. Flap threaded insert
2. Vertical control bar
3. Bar guide
4. Fork
5. Crank
6. Switcher
7. Engine arm
8. Engine
9. Motor base
10. Motor cover
11. Mechanical docking plate
12. First horizontal bar
13. Offset
14. Second horizontal bar
15. Bar driving
16. Sensors
17. Transmission fork
18. Bugs cam
19. Wand coupling
20. Wand
21. Spoon

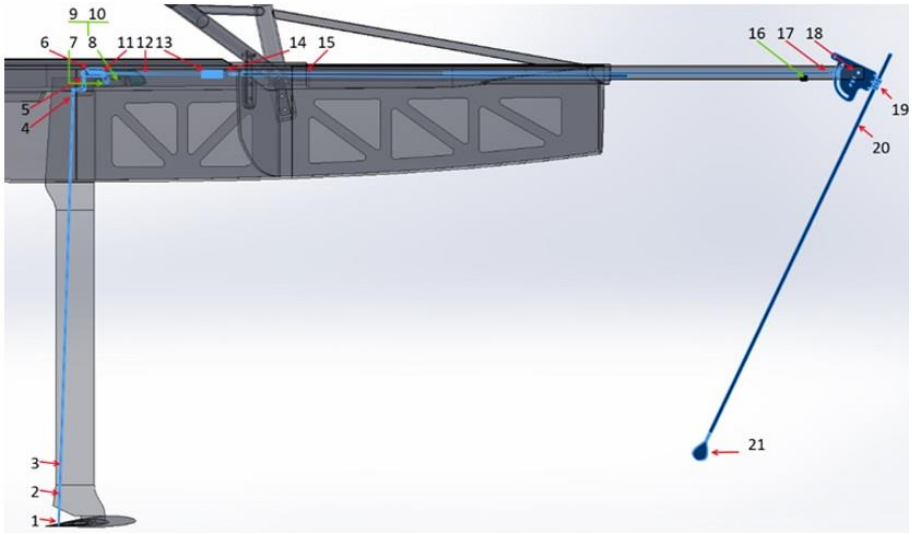


*Figure 1-29: Control system's overview*

Starting from the foil, there is a threaded insert (1) which is laminated into the foil flap and connects to the thread of the vertical bar (2) of the centreboard which slides into the bar guide (3) laminated inside the centreboard. On the other side, the bar is connected to the transmission crank (5) through a fork (4). The transmission crank is clamped in the centre by a pin that is connected to an insert laminated into the centreboard.
The transmission crank is connected to the **shifter** (6). It can be interfaced with the electronic system rather than the mechanical one in simple and user-friendly operations. Both systems have a connection element, for the motor it is an arm (7) connected to the motorized system (8), for the mechanical system it is a perforated plate (11) connected to the first horizontal bar (12). The electronic system is connected to the deck by a base (9) and is protected by a cover (10).
The mechanical system continues with the first horizontal bar which fits into the offset (13), which is an adjustment element. The second bar (14) is connected on the other side of the offset and goes to bugs cam (18) passing inside the tree foot and into a channel (15) that controls the bending deformation of the INOX bar. At the interface between the bugs cam and the fork (17) there is a roller which slides in the designed guide of the bugscam. Connected to the bugs cam there is a holder (19) for the wand (20) into which it can slide. The wand has a spoon at its end (21) that can bounce continuously on the water.

# 2 Manufacturing and cost analysis


*Figure 2-1: Foils' lamination*

## 2.1 Hull, deck, deckhouse

After the milling and assembly of both the hull and deck moulds, preparation for the lamination began. This process included applying ultrafine polyester putty to smoothen the surfaces and close any gaps that resulted from the assembly of the milled components, applying various layers of epoxy resin to impermeabilize the structures, two layers of **primer** and two layers of gelcoat. A water-based **release** agent was then applied to all surfaces.

Once the moulds were ready to be used, the lamination phase began, opting for a hand layup technique, where, in order to reduce waste and increase quality, all basalt fibres were separately impregnated with epoxy resin then positioned onto the mould one by one. This included the positioning of the core of both parts.
Once the lamination came to an end, both moulds were vacuum sealed. This step proved to be extremely successful. The pressure held by both moulds was optimal, showing not only the result of a proper preparation of the moulds themselves prior to the lamination, but also their strength. Additionally, the surface finish was uniform, proof that the vacuum was also well distributed along the entire laminate.

After curing and hardening of the laminate the removal of the two components from their respective moulds started. At this point, the releasing agent used in the preparation phase of the moulds was not as efficient as expected, resulting in damages on both moulds, and superficial imperfections on the laminates themselves.
This, however, did not compromised the quality of either laminates.

*Figure 2-2: Deckhouse lamination*

As far as the manufacturing of the deckhouse is concerned, an economic and manual approach was conducted. First of all, the designing of a CAD model of the part based on the assembly. Then a mould was designed on the outside of the surface with five sections. From this CAD the 2D jigs of sections and surfaces have been printed.

So, instead of milling the pieces they were cut by hand from reused wood: compressed wood for the base and the sections and plywood for the laminated surface. Once all the parts were ready, they were put together with some nails and prepared the mould with epoxy resin and wax for releasing.
At the end, the lamination of the deckhouse on this mould occurs with **basalt fibre** (2 plies twill and UD ply for reinforcement), a core of cork and epoxy resin. Finally, vacuum was used to consolidate the part.

## 2.2 Appendages

Starting from the critical issues encountered during the last SuMoth edition, few guiding points were defined to lead the design phase in accordance with the production and manufacturing processes that are available to our team:

- **Greater dimensions** in order to obtain greater control over lamination quality, and to allow for a more manageable and precise positioning of all necessary internal components, further allowing for a fluid and correct functioning of the control system mechanism;
- The use of a different method for the insertion of all threaded inserts, which showed to be fundamental in the coupling of the vertical and horizontal centerboard components;
- The use of an extruded carbon duct to guide the steel beam in the vertical component, used to control the movement of the foil flap;
- The use of expanding epoxy foam as a component filler.

It is important to note that the vertical and horizontal components of the centerboard were each made by combining two valves, each laminated separately.

### 2.2.1 Production of vertical centreboard component

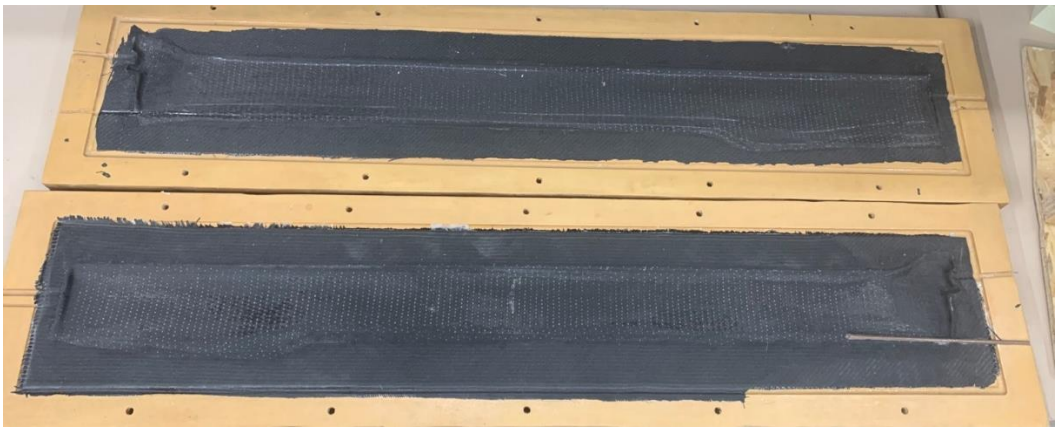

*Figure 2-3: Vertical Centreboard after lamination*

After a meticulous design phase, and the production of the moulds optimized in accordance with production requirements, the manufacturing of the appendage itself began through a hand layup lamination process. In pursuance of the most optimal result, multiple layers of releasing agents were applied: two layers of PVA release film, and two layers of releasing wax. To facilitate the reduction of waste material, customized templates were used during the cutting of the various carbon fibers that were then used during the lamination.
The various carbon fiber skins were impregnated with resin on a separate table, and not directly on the moulds, facilitating quality checks and the removal of any excess resin, thus optimizing the lamination process as much as possible.

After this procedure, and after a layer of epoxy resin was applied to the mould, each layer was then placed into said mould.
At the end of the cure and hardening phase of the laminate the following step included the insertion of all fundamental pieces for the functioning of the control system and the coupling of the two vertical and horizontal components.
This included the fixing of the threaded insert and the carbon duct for the control system beam. To ensure the correct positioning of these components, expanded polyurethane foam was used to produce supports to fix these into one of the laminated valves. Furthermore, the same material was used to produce a wall placed horizontally on the valve. The reason why this was done was to prevent any expanding epoxy foam from invading the upper section of the vertical centerboard component, where the mechanism that moves the steel beam inside the carbon duct (which, in turn, as a result of impulses from the control system, moves the flap of the foil) was placed. These support structures were then glued to the laminated component using loaded resin.
The same loaded resin was used for gluing the two valves, during which the expanding foam was also inserted for filling.
Once the hardening time had elapsed, the excess flanges were removed, and the component was polished.

### 2.2.2 Production of horizontal component

*Figure 2-4: Foil joint*

The production technology used for this process was the same as previously described for the vertical component. This includes the preparation of the moulds prior to hand layup lamination. However, the presence of substantial differences between the two components allowed the utilization of a different production process. The absence of mechanical systems within the horizontal component eliminated the need for any support structures, unlike the vertical component.
The presence of a **"female" joint** made it necessary to laminate this section of the component separately from the rest of the valve. This was done prior to the complete lamination process, then inserted to complete the component during the lamination. Note that to avoid any air bubbles between the hardened laminate and the wet resin impregnated fibers (which would have caused structural complications) the first layer was cut in accordance with the joint edges, leaving the previously laminated piece as a "first layer" in said restricted area. To further avoid this, carbon rowing was applied around the joint.

After the lamination, the gluing and filling phase started, where a thin layer of Kevlar was placed between the two valves. This, after the hardening process, facilitates the fluid movement of the flap.
After trimming the excess flanges and polishing, the horizontal component was then drilled in accordance with the joint in order to allow the passage of the tightening screw that then goes into the threaded insert in the corresponding position in the vertical component.
A threaded insert has been positioned within the flap to allow a fixed connection between the steel beam in the vertical component and the flap itself.
Finally, the layer of Kevlar was cleaned of all resin and carbon, and coated with a thin layer of protective Sikaflex.

## 2.3 Wings

The material chosen for the wing's bars are old and broken windsurf masts to give them a "second life". The bars are connected in the corners with junctions milled with Hull mould scraps so that they could be clean and good-looking too.

## 2.4 Main foil control system

Reference the following figure, previously presented in the design section, the main components of the system are described.

1. Flap threaded insert
2. Vertical control bar
3. Bar guide
4. Fork
5. Crank
6. Switcher
7. Engine arm
8. Engine
9. Motor base
10. Motor cover
11. Mechanical docking plate
12. First horizontal bar
13. Offset
14. Second horizontal bar
15. Bar driving
16. Sensors
17. Transmission fork
18. Bugs cam
19. Wand coupling
20. Wand
21. Spoon

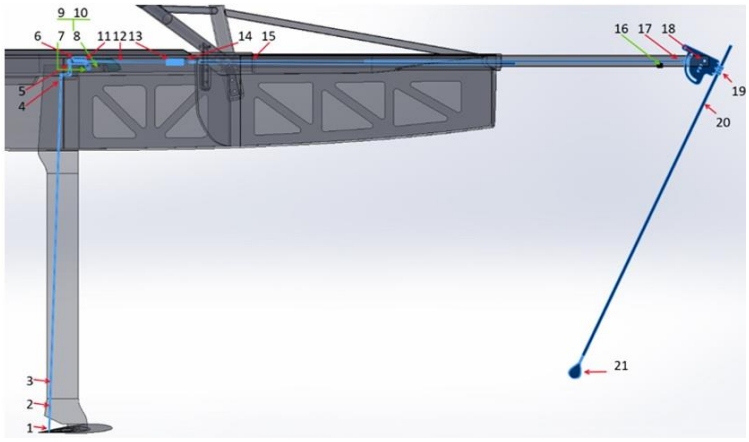


*Figure 2-5: control system's components*

1) **Flap threaded insert** M3. It is inserted and glued into a hole on the flap and respects the designed 35 $mm$ arm to the flap pivot.

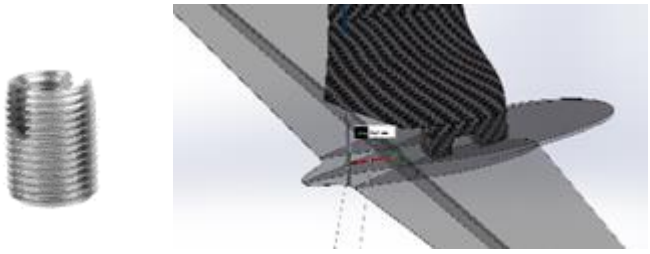

*Figure 2-6: Flap threaded insert*

2) Stainless steel vertical bar of 3 $mm$ diameter with thread on both sides to connect to the flap insert on one side and to the fork on the other side

3) Bar guide. Carbon tube $d_{int} = 3mm \;\; d_{est} = 5mm$. It is laminated between the two valves of the vertical and is tilted of 2 ° to permit the correct inclination of the bar in order to connect with the transmission crank.

4) Aluminium fork allows vertical bar length adjustment. Creates an adjustment between crank and flap angle.

5) **Crank**. Made of stainless steel from a 5$mm$ laser-cut sheet and lightened in the area of connection with the fork by 3$mm$. The complete angular excursion of the crank around the hinge has been appropriately evaluated in order to limit the deflection of the vertical bar inside the centreboard and optimise the horizontal excursion of the motion imposed by the mechanical system. The connection in the hinge is made with a through-hole in the centreboard with a screw in one end that is countersunk and connects to the other end in an insert like the first.

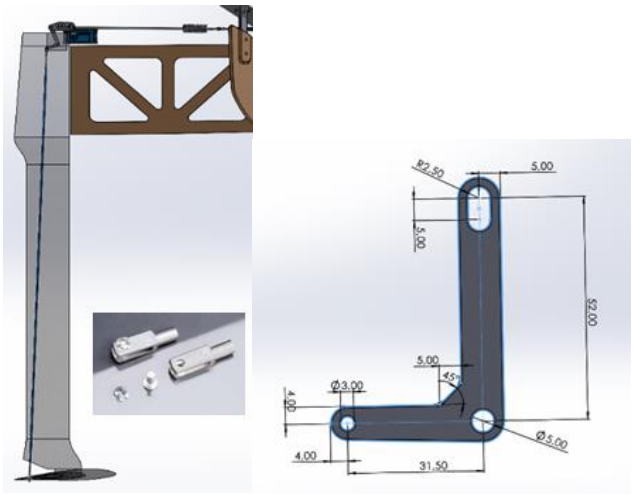


*Figure 2-7: cranck*

6) **Switcher**. A vernier adjuster connected on one side to the crank, on the other it allows connection to both the mechanical and electronic systems, creating two stable kinematics capable of transmitting the necessary motion to the crank and thus to the flap. The connection is made by pins which lock two holes in a plate (11) holed and welded onto the bar in the mechanical control, while in the electronic control a pin is connected to the arm (7) of the motor. This system was designed with the aim of making it possible for the sailor to interface quickly and conveniently with the two control systems. In fact, with a few movements he/she is able to switch from one to the other and be able to take advantage of two distinctly different sets of control logics and racing tactics.

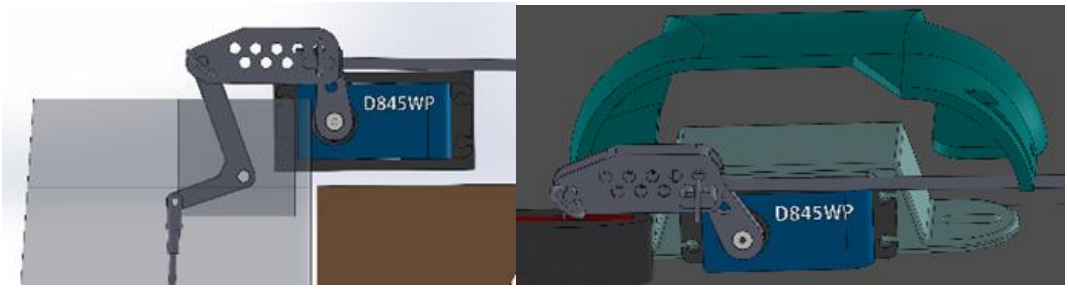


*Figure 2-8: Switcher*

8) **Servo motor**. High-torque servo motor, a rotary actuator that allows precise control of angular or linear position, velocity and acceleration. It is controlled varying the duty cycle of a PWM signal: depending on this, the servo is able to move and change the angle of his arm. It is capable of delivering $50kg/cm$ of torque with a total weight of $227g$. Concerning the water resistance level, it has obtained the IP67 certification.

9) Motor base. Made in 3D from completely recyclable pet material, it allows to couple the engine in axis with the shifter and thus with the crank and the daggerboard, unloading the moments generated onto the deck. It is connected to the deck by threaded inserts inserted in holes in the deck and suitably laminated to ensure the system is waterproof and watertight. There are loops that allow deviations of a few millimeters in order to better set the interface of the electronic system with the appendage.

10) Motor cover. The design of the motor cover allows it to be protected from knocks and contributes to the functionality of the control system. In fact, it has a guide that offers a stability link to the first bar when it is in operation under the drive of the automatic mechanical system and allows it to be disengaged when the

mechanical system is disconnected by positioning it in a non-obstructive disengagement zone for the electronic system.

13) **Offset.** The offset allows adjustment of the horizontal length of the control system, by interfacing with the crank and the bugscam guide. It has coils on which a rope, looped several times, creates a circuit capable of changing the length of the bars that relate to the crank and bugs cam. The offset circuit is closed: it rotates around the offset, arrives at the terraces by passing through a pair of eyes, passes under the terraces and then returns to the offset. The circuit must be very tensioned and squeezed, so that the offset remains stationary in the position chosen by the sailor in line with the adjustment logic. It is $60mm$ long, has $3mm$ pitch and has $19$ windings in which a rope with a maximum diameter of $2.5mm$ can run. Of the $19$ windings, we can keep $3-4$ always occupied by the line to provide a strong grip and smooth movement. With a slide at each turn of the offset, the horizontal line is lengthened by $0.8mm$ for a total of $12mm$ in $15$ turns. We designed two models: with one slide and with two slides in which we double the variation of the horizontal stretch.

| | |
|---|---|
| Length | $60mm$ |
| External diameter | $24\ mm$ |
| External pitch | $3mm$ |
| N. windings | 19 |
| Internal diameter | $5.5\ mm$ |
| Nut diameter | $M5$ |
| Nut pitch | $0.8mm$ |
| Rod diameter stainless steel 304 | $M5$ |

*Table 2-1: Offset dimensions*

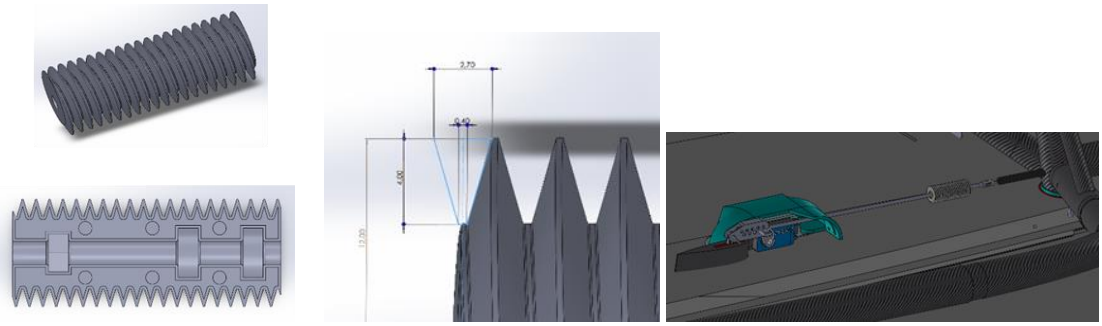

*Figure 2-9: Offset component*

12,14) Stainless steel bars. Bar diameter $5\ mm$ maximum length $3m$ threaded M5 at the ends. The threading makes it possible to recover any lengths in the entire horizontal section from the crank to the bugscam through the 5mm stainless steel forks (17).

15) Bar driving. Carbon channel outer diameter 10mm, inner diameter 5mm controls the deflection of the steel rod and drives it from the mast foot to the end of the bowsprit.

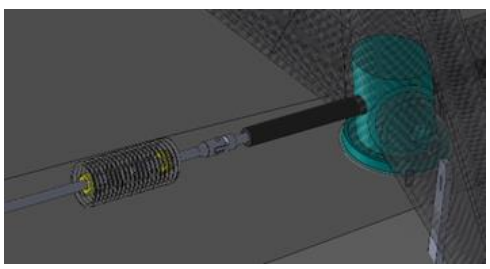

*Figure 2-10: Bar driving*

16) **Ultrasonic sensor**. The ultrasonic sensor uses sonar to determine the distance from an object. The ultrasound transmitter emits a high-frequency sound, it travels through the air and, if it finds an object, it bounces back to the module. The ultrasound receiver detects the reflected sound. The time between the transmission and reception of the signal allows us to calculate the distance to an object. This is possible because we know the sound's velocity in the air.

18) **BugsCam**. It is constructed of stainless steel and weighs just over $300\ g$. It is the core part of the control system and was designed down to the smallest detail to ensure that the transmission of motion recorded by the wand will transfer the necessary lift information to the flap at the bottom of the centerboard. It is hinged by an 8mm pin passing through the bowsprit and is held in the vertical plane by grooves on the bowsprit that absorb moments around different axes. The connection with the fork is in tolerance on the side faces so as to transmit any inclinations to the rod to which the fork is connected. The bar is clamped to remain on axis by a plate that absorbs any torsion of the bugscam and fork. This allows to the bugscam to move smoothly with respect to the roller running in its guide.

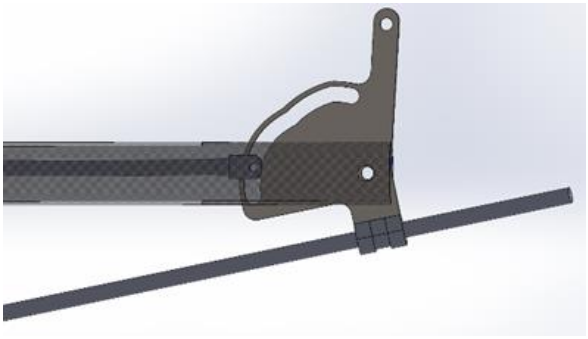

*Figure 2-11: BugsCam CAD*

19) Wand coupling and wand length regulation. Thanks to this coupling, which is inclined by a few degrees, the wand can make its full rotation without bumping into the hull. In addition, thanks to a ring, the wand's length adjustment circuit is created, which allows for the variation in sensitivity of the boat.

20) Wand and spoon. $10mm$ diameter hollow carbon bar, at the bottom of which a spoon is laminated with recovered material from lamination of appendices.

*Figure 2-12: Wand and spoon*

# 3 Sustainability analysis

## 3.1 General description

We focused on the impact reduction both at the beginning and at the end of the boat production life cycle. For this reason we chose materials with a lower production impact, for example the basalt fibre impacts less than the glass fibre. The core is made with balsa wood as later better explained in the LCA report.
We also used **Okume wood** that has a lower impact with respect to other epoxy composites, we chose a recycled PET instead of a virgin one and our resin is completely recyclable.

## 3.2 Boat and elements lifecycle

As previously mentioned in the hull mould section the impact of the manufacturing of the hull and deck moulds is minimised, thanks to the meticulous attention on the material used and its quantity: the moulds were made with expanded polyurethane foam with density $120\ Kg/m$ since using denser foams would have affected excessively our SM$ budget. This choice is not the best one since this type of material is quite polluting, but because of time constraints it was forced for shipping reasons, since a delay could have compromised the attendance at the competition.
However, with more time, a better tooling board could have been used, such as recycled polyurethane foam or biobased ones. An example of good alternative could be [6].
At the end of its life the team is planning to execute a **chemical recycling** and recovery of fibres after the internal structure removal. In particular, through the solvolysis process it is possible to clean and recover the fibres used as composite reinforce. Recovered fabrics may be re-laminated for other smaller parts and applications, or re-melted in case of basalt fibres. As the boat ages, a suitable solution may be its refitting and replacement of broken parts in order to make it suitable to sail for many more years to come.

Moreover, the team is still considering the possibility of manufacturing a set of foils in basalt fibre and carbon, to have the chance to chemically dissolve polymeric matrix and recover the woven fabrics.
As previous said, in order to be more sustainable we settled for the re-use old windsurf mast as tubes for our wings' bars, while regarding smaller elements of the boat, they could be re-used in other team's current projects.

## 3.3 Action for sustainable future

Recycling and reducing wastes must be a social priority that everyone should follow. Research in new bio-based composites is definitely something worth investing. Natural fibres as reinforce, such as basalt, require less energy to be produced and do not require additives.
Also, the use of a bio-based matrix, with a reduced percentage of fossil carbon may reduce the environmental impact. Upcycling is also an important step that reduces the production of new materials by reusing a modified version of the old components, cutting off wastes considerably. Reducing spray paint, and carbon fibre and resin waste as much as possible is what we can improve the most on as a university team.

Further, working in additive can be a solution as 3D printing is much more efficient than injection moulding.
Leaving aside the sail world, to reduce pollution due to cargos or cruise ships, the strategy that is being adopted is to use less-harmful fuels for ship engines. The International Maritime Organization (IMO) has delineated several Emission Control Areas (ECAs), the Baltic Sea area, the North Sea area, the North American area and the Unites States Caribbean Sea area, where ships must use more expensive low-sulphur fuel because they tend to concentrate their activities in specific coastal areas, creating a significant cumulative impact at the local scale.

# 4 Marine Shift 360 LCA

Our team has always been focused on the environment, seeking to optimise each of our processes for more sustainable production. Fundamental to this is the use of LCA analysis, a quantitative and objective methodology that allows the environmental impacts of processes to be analysed using standardised software.
In this analysis, the '**Marine Shift 360**' software was used, enabling a life cycle assessment using databases specific to the marine industry, promoting sustainable development and comparing possible technical solutions.
We were able to obtain further information on the materials with the worst environmental impact, in order to investigate new process methods to reduce their impact.
In the planning of the project, we focused on the use of recycled materials: a striking example of these are the wings, which were made from windsurfing tubes already in stock.

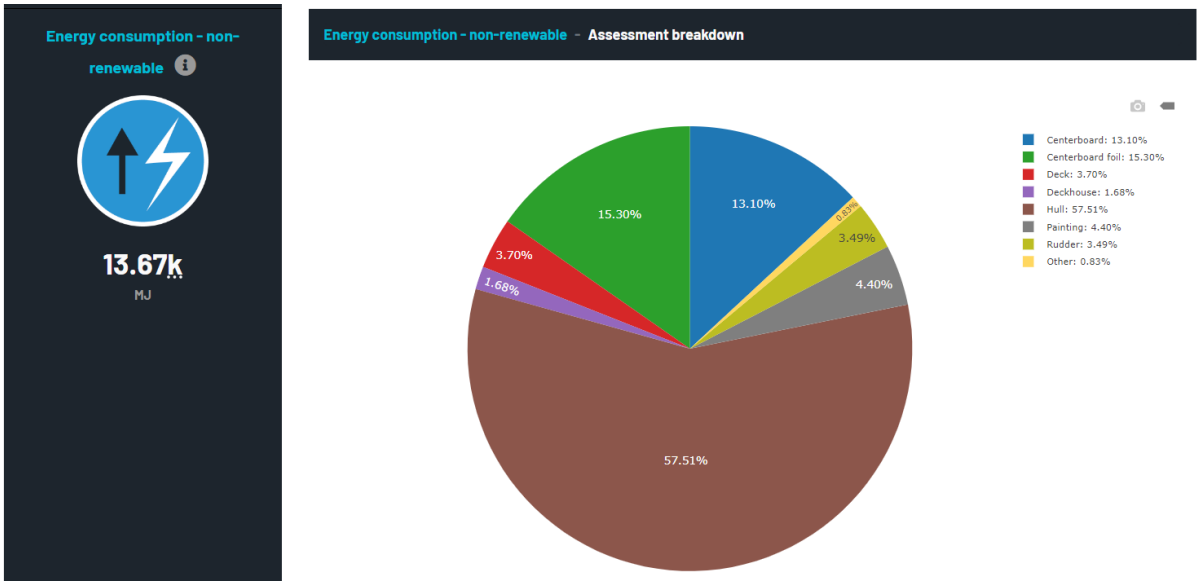


*Figure 4-1: energy consumption non-renewable*

The consumption of energy from non-renewable sources, in any process, accounts for a preponderant portion of $CO2_{eq}$ emissions and is strongly influenced by the geo-location of the process, as each state uses its own energy mix. Specifically, as can be seen from the graph, 75% of the energy we consume is from the use of the CNC milling machine to shape the hull's mould. To try and minimise this we did not mill from solid material but composed the blank from many small blocks. This process also allowed us to minimise both the volume of materials used and the production time, which specifically took about a month. As for the actual lamination of the hull, this was done by hand: the skins used were basalt TWILL with UD $200 - 300 g/m^2$ reinforcements; the core is composed of balsa with steel plate reinforcements. The reinforcements and core were prepreg-laminated, while the twill was dried and sprinkled with resin on the mould itself. To conclude, we laid out peel-ply, micro-perforated and absorbent and pulled the vacuum with a vacuum machine.

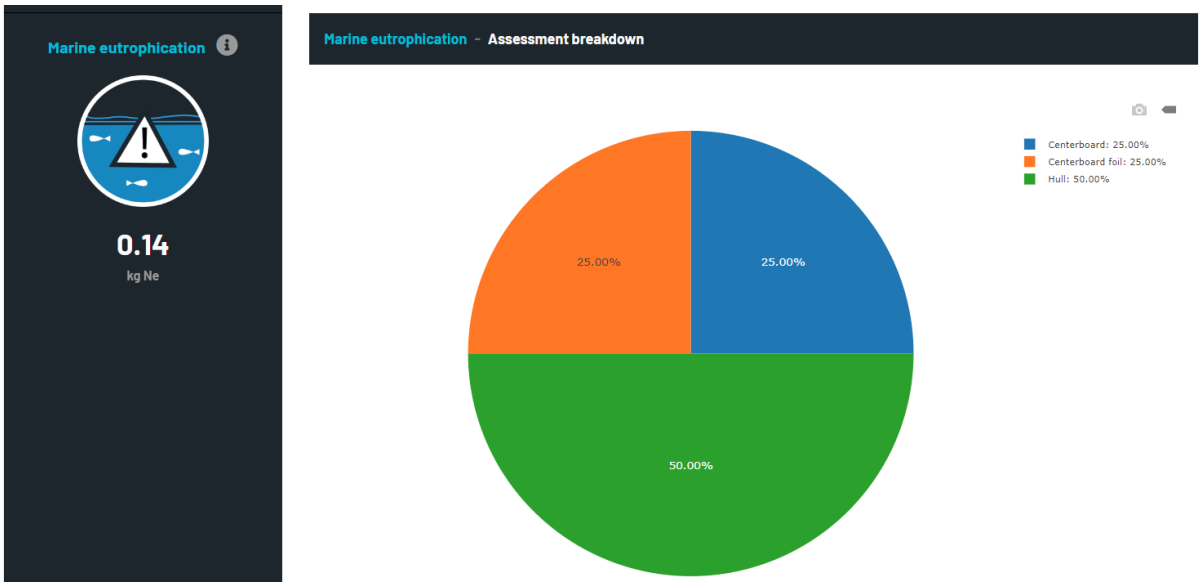


*Figure 4-2: Marine eutrophication*

As we can see from the graph, eutrophication is an impact class that does not particularly affect our process: thanks to a careful choice of process methods and an optimal selection of the materials used, we have managed to minimise the emission of nitrates and phosphates. By doing so, we achieve a very low impact on the biophysical economy of our territory, characterised by the presence of a very important watercourse such as the Po, which is already endangered by strong industrial activity.

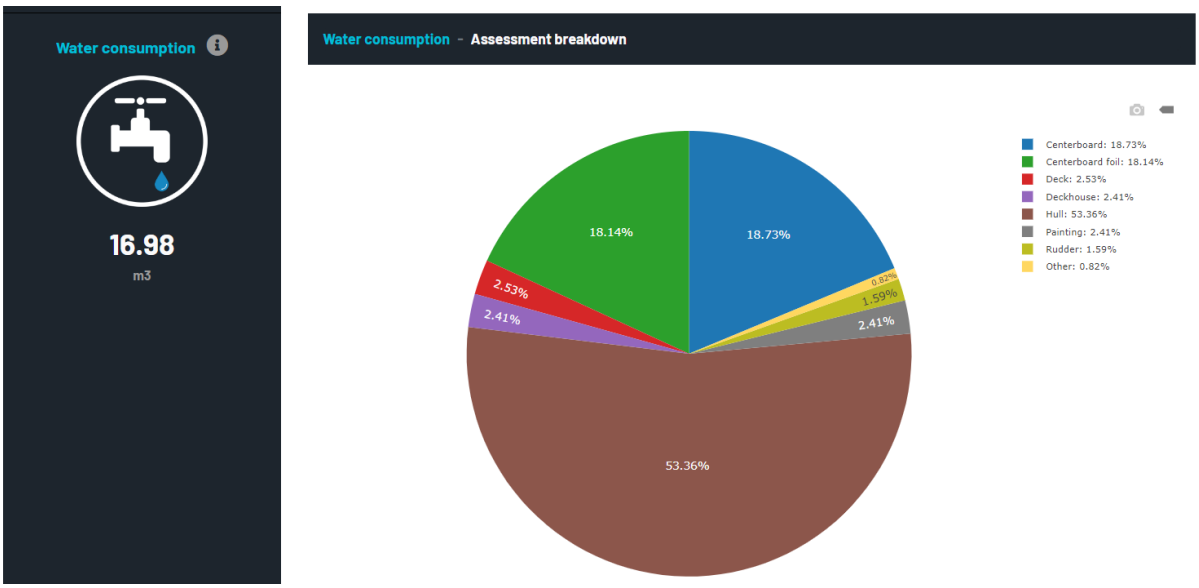


*Figure 4-3: Water consumption*

Such high water consumption is mainly rooted in the balsa wood: being wood derived from a tropical tree, water consumption increases considerably. Given the extreme usefulness and efficiency of this type of wood, it was decided to continue using it, but to optimise the entire production process in order to save as much water as possible. For example, we saved a large amount of water in the creation of the deckhouse, as can be seen from the graphs: it was obtained from the balsa waste from the hull and deck work.

An advantageous characteristic of balsa is that it has a positive Carbon Footprint, a fact that should not be overlooked when choosing a construction material. Indeed, balsa wood is a sustainable material given the carbon sequestration potential of balsa trees and the carbon offset value at the end of any product made from balsa wood.

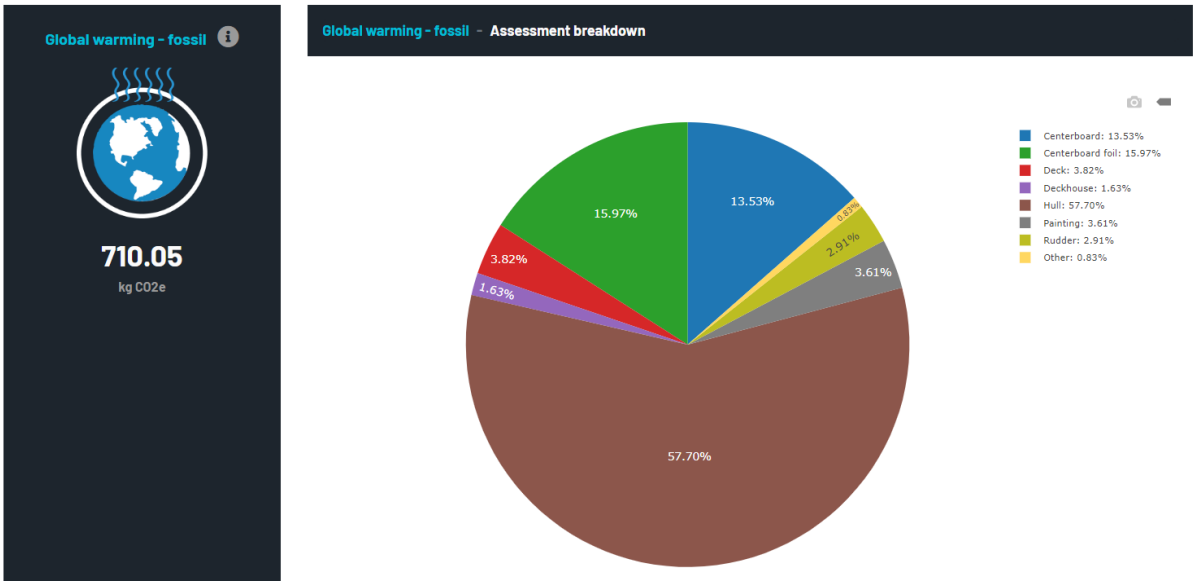


*Figure 4-4: CO2 emissions*

The CO2 emission study of our process encapsulates all the information described above. It can be noted that the most impactful element is the production of the hull and its mould, as it is the key work phase of our process, i.e. the one that consumes the most material and electricity.
We have tried to minimise electricity consumption as much as possible by optimising work shifts and the use of the most impactful equipment, through the methodologies described in the energy consumption analysis. In addition, this year, our team invested heavily in research trying to develop innovative recycling methods.

# 5 Bibliography


[1] https://www.boatdesign.net/attachments/foils-moth-thesis-boegle-pdf.77496/Dfbdxbd
[2] https://www.boatdesign.net/attachments/beaver-paper-on-moth-pdf.139227/
[3] https://odr.chalmers.se/bitstream/20.500.12380/301921/1/Rapport%20FINAL%20Albin%20Boman.pdf
[4] https://avalonsails.com.au/blog/2018/3/14/latest-update-on-the-bugs-cam
[5] https://www.advancedwingsystems.com/
[6] https://compositesuk.co.uk/communication/news/ru-bix-launch-new-sustainable-and-hybrid-tooling-board-ranges

**Professor:** Giuliana Mattiazzo (**Team Manager**)
**Team Leader:** Alessandro Cogo

**Product Manager:** Lorenzo Collo (**Team Captain**)
**Project Manager:** Carolina Cipriani (**Communications Officer**)


**Manufacturing Section**
Alessandro Lombardo
Vincenzo Di Vincenzo
Leonardo Romano
Bruna Di Dato
Davide De Martino
Francesco Mazzoli
Lorenzo Bonelli
Marius Paksys
Domenico Prestanicola
Gianluca Bologna
Filippo Boukas
Alberto Cavallero

**Management Section**
Mattia Santarosa
Luca Lamberti (**Logistics Officer)**
Marco Vincenti
Valentina Di Domenico

**Sailors Section**
Carolina Foroni
Lorenzo Collo

**Foils Section**
Leonardo Stumpo
Giuseppe Monaco
Pietro Surico
Marco Lalloni
Francesco Bandinelli
Luca Batignani
Margherita Aragona
Enrico Scribano
Gabriele Campana
Simone Pintaldi
Simone Dei Rossi
Paul Russell Lancry

**Control System Section**
Gabriele Deflorio
Alessandro Landra
Gaia Morici
Tommaso Pantano
Simona Cundari
Paolo Cesano
Gian Paolo Sellitto
Andrea Baglieri

**Architecture Section**
Salvatore Bucaria
Daniele Poggio
Sara Montagner
Riccardo Negro
Luca Cattarossi